



Chemical and
physical controls on
pollution transport to
the Arctic

S. A. Monks et al.

This discussion paper is/has been under review for the journal Atmospheric Chemistry and Physics (ACP). Please refer to the corresponding final paper in ACP if available.

Multi-model study of chemical and physical controls on transport of anthropogenic and biomass burning pollution to the Arctic

S. A. Monks¹, S. R. Arnold¹, L. K. Emmons², K. S. Law³, S. Turquety⁴,
B. N. Duncan⁵, J. Flemming⁶, V. Huijnen⁷, S. Tilmes², J. Langner⁸, J. Mao⁹,
Y. Long⁴, J. L. Thomas³, S. D. Steenrod⁵, J. C. Raut³, C. Wilson¹,
M. P. Chipperfield¹, H. Schlager¹⁰, and G. Ancellet³

¹Institute for Climate and Atmospheric Science, School of Earth and Environment, University of Leeds, Leeds, UK

²National Center for Atmospheric Research, Boulder, Colorado, USA

³UPMC Univ. Paris 06, Univ. Versailles Saint-Quentin, CNRS/INSU, LATMOS-IPSL, Paris, France

⁴Laboratoire de Météorologie Dynamique, IPSL, CNRS, UMR8539, 91128 Palaiseau Cedex, France

⁵NASA Goddard Space Flight Center, Greenbelt, USA

⁶European Centre for Medium range Weather Forecasting, Reading, UK

Title Page

Abstract

Introduction

Conclusions

References

Tables

Figures



Back

Close

Full Screen / Esc

Printer-friendly Version

Interactive Discussion



⁷Royal Netherlands Meteorological Institute (KNMI), De Bilt, the Netherlands

⁸Swedish Meteorological and Hydrological Institute, 60176 Norrköping, Sweden

⁹Program in Atmospheric and Oceanic Sciences, Princeton University and Geophysical Fluid Dynamics Laboratory/National Oceanic and Atmospheric Administration, Princeton, New Jersey, USA

¹⁰Deutsches Zentrum für Luft- und Raumfahrt (DLR), Institute of Atmospheric Physics, Oberpfaffenhofen, Germany

Received: 30 June 2014 – Accepted: 8 September 2014 – Published: 2 October 2014

Correspondence to: S. A. Monks (s.a.monks@leeds.ac.uk)

Published by Copernicus Publications on behalf of the European Geosciences Union.

Chemical and physical controls on pollution transport to the Arctic

S. A. Monks et al.

Title Page

Abstract

Introduction

Conclusions

References

Tables

Figures



Back

Close

Full Screen / Esc

Printer-friendly Version

Interactive Discussion



Abstract

Using observations from aircraft, surface stations and satellite, we comprehensively evaluate multi-model simulations of carbon monoxide (CO) and ozone (O₃) in the Arctic and over lower latitude emission regions, as part of the POLARCAT Model Inter-comparison Project (POLMIP). Evaluation of eleven atmospheric models with chemistry shows that they generally underestimate CO throughout the Arctic troposphere, with the largest biases found during winter and spring. Negative CO biases are also found throughout the Northern Hemisphere, with multi-model mean gross errors (9–12%) suggesting models perform similarly over Asia, North America and Europe. A multi-model annual mean tropospheric OH ($10.8 \pm 0.6 \times 10^5 \text{ molec cm}^{-3}$) is found to be slightly higher than previous estimates of OH constrained by methyl chloroform, suggesting negative CO biases in models may be improved through better constraints on OH. Models that have lower Arctic OH do not always show a substantial improvement in their negative CO biases, suggesting that Arctic OH is not the dominant factor controlling the Arctic CO burden in these models. In addition to these general biases, models do not capture the magnitude of CO enhancements observed in the Arctic free troposphere in summer, suggesting model errors in the simulation of plumes that are transported from anthropogenic and biomass burning sources at lower latitudes. O₃ in the Arctic is also generally underestimated, particularly at the surface and in the upper troposphere. Summer O₃ comparisons over lower latitudes show several models overestimate upper tropospheric concentrations.

Simulated CO, O₃ and OH all demonstrate a substantial degree of inter-model variability. Idealised CO-like tracers are used to quantitatively compare the impact of inter-model differences in transport and OH on CO in the Arctic troposphere. The tracers show that model differences in transport from Europe in winter and from Asia throughout the year are important sources of model variability at the Barrow. Unlike transport, inter-model variability in OH similarly affects all regional tracers at Barrow. Comparisons of fixed lifetime and OH-loss idealised CO-like tracers throughout the Arctic

Chemical and physical controls on pollution transport to the Arctic

S. A. Monks et al.

Title Page

Abstract

Introduction

Conclusions

References

Tables

Figures



Back

Close

Full Screen / Esc

Printer-friendly Version

Interactive Discussion



Chemical and physical controls on pollution transport to the Arctic

S. A. Monks et al.

[Title Page](#)[Abstract](#)[Introduction](#)[Conclusions](#)[References](#)[Tables](#)[Figures](#)[Back](#)[Close](#)[Full Screen / Esc](#)[Printer-friendly Version](#)[Interactive Discussion](#)

troposphere show that OH differences are a much larger source of inter-model variability than transport differences. The concentration of OH in the models is found to be correlated with inter-model differences in H_2O , suggesting it to be an important driver of differences in simulated concentrations of CO and OH at high latitudes in these simulations. Despite inter-model differences in transport and OH, the relative contributions from the different source regions (North America, Europe and Asia) and different source types (anthropogenic and biomass burning) are comparable across the models. Fire emissions from the boreal regions in 2008 contribute 33, 43 and 19 % to the total Arctic CO-like tracer in spring, summer and autumn, respectively, highlighting the importance of boreal fire emissions in controlling pollutant burdens in the Arctic.

1 Introduction

During the 20th century, regions poleward of 60°N have warmed at a rate 50 % greater than the Northern Hemisphere (NH) average ($0.09^\circ\text{C decade}^{-1}$ compared to $0.06^\circ\text{C decade}^{-1}$) (ACIA, 2005). This is due to feedback mechanisms, such as the snow and sea-ice-albedo feedback, where melting ice leads to increased absorption of solar radiation, which further enhances warming in the Arctic (Serreze and Francis, 2006). Studies have shown that Arctic temperatures respond to both local and non-local radiative forcing, meaning that reducing emissions of greenhouse gases and their precursors throughout the Northern Hemisphere will be beneficial in slowing Arctic warming (Shindell, 2007). Shindell and Faluvegi (2009) estimated that anthropogenic emissions of black carbon (BC) and secondary production of tropospheric ozone (O_3) from anthropogenic precursor emissions have contributed 0.5–1.4 and 0.2–0.4 $^\circ\text{C}$ to Arctic warming since 1890, respectively. The short lifetimes of these species compared to carbon dioxide (CO_2), mean that emission reduction measures that target these species in conjunction with CO_2 could offer a more immediate abatement of climate warming than measures targeting solely CO_2 (Quinn et al., 2008). Consequently,

Chemical and physical controls on pollution transport to the Arctic

S. A. Monks et al.

Title Page

Abstract

Introduction

Conclusions

References

Tables

Figures



Back

Close

Full Screen / Esc

Printer-friendly Version

Interactive Discussion



wet deposition during long-range transport. This was demonstrated by Shindell et al. (2008) who examined source contributions from different NH anthropogenic emission regions to Arctic burdens of sulphate, BC, CO and O₃ and found that sulphate and BC were mostly sourced from Europe, in agreement with previous studies. However, for CO and O₃, North America, Asia and Europe were all shown to be important throughout the year, with North America dominating the O₃ burden and Europe dominating the CO burden.

The sensitivity of the Arctic to different source regions is related to their regional export efficiencies and boundary layer export mechanisms. Stohl (2006) used a Lagrangian model to study seasonal transport to the Arctic from North America, Europe and Asia and identified three main pathways that varied in terms of importance depending on the source region and season. These were low-level transport followed by ascent in the Arctic, low-level transport alone, and uplift outside the Arctic followed by descent within the Arctic. Stohl (2006) showed that European emissions could follow all three pathways, however, North American and Asian emissions tended to follow the latter. Asia and North America are ideally located to allow frequent rapid transport from the boundary layer into the free troposphere by warm conveyor belts, which occur ahead of a passing cold front (Stohl, 2001). In contrast, warm conveyor belts are not as common over Europe, and export of emissions occurs mostly at low-levels (Stohl, 2001; Duncan and Bey, 2004; Eckhardt et al., 2004). These different transport pathways result in a vertical gradient in Arctic sensitivities to different emission regions, with the higher altitudes being more sensitive to emissions from North America and Asia and the lower altitudes being more sensitive to emissions from Europe and Siberia (Klonecki et al., 2003).

Long-term changes in regional emissions may also be important in determining the relative contributions to Arctic pollutant burdens. Arctic surface observations showed a decrease in O₃ concentrations during the 1980s to the mid-1990s and a small increase afterwards (Oltmans et al., 1998, 2006; Helmig et al., 2007). In addition, Arctic CO surface measurements showed a downward trend during the late 1980s and early

Chemical and physical controls on pollution transport to the Arctic

S. A. Monks et al.

Title Page

Abstract

Introduction

Conclusions

References

Tables

Figures

◀

▶

◀

▶

Back

Close

Full Screen / Esc

Printer-friendly Version

Interactive Discussion



5 a loss of HO_x from the atmosphere, needs to be included in models in order to increase concentrations of winter/spring CO. The generally poor skill and large variability of global models in simulating Arctic burdens of these species has implications for our confidence in a model's ability to accurately simulate climate responses to changes in mid-latitude emissions. Therefore, there is a need to better understand the chemical and physical processes that lead to these model differences and biases.

10 An improvement in this understanding is largely limited by a paucity of observations of chemical constituents throughout the Arctic troposphere, particularly away from the surface, where enhancements from more southerly sources in North America and Asia are more likely to be found (Klonecki et al., 2003). The POLARCAT (POLar study using Aircraft, Remote Sensing, surface measurements and models of Climate, chemistry, Aerosols, and Transport) campaign intensively sampled the Arctic and sub-Arctic during spring and summer 2008, as part of the International Polar Year (Law et al., 2014). The POLARCAT Model Intercomparison Project (POLMIP) aims to exploit this observational dataset to evaluate models in the Arctic and sub-Arctic (Emmons et al., 2014). In this study, we use POLMIP simulations of CO, O₃ and OH in conjunction with POLARCAT aircraft observations, surface measurements and satellite observations, within the Arctic and near source regions to evaluate model performance (Sect. 4). The availability of the aircraft observations in the Arctic allows a more extensive multi-model evaluation of models within a variety of air-mass types in the Arctic than previously undertaken. Idealised tracers are used to provide a useful summary of the relative importance of anthropogenic and biomass burning sources from several models throughout the year 2008 and to investigate inter-model differences in these source contributions (Sect. 5). The aim of this paper is to provide a better understanding of inter-model differences in simulated Arctic trace gases.

20

25

Chemical and physical controls on pollution transport to the Arctic

S. A. Monks et al.

[Title Page](#)[Abstract](#)[Introduction](#)[Conclusions](#)[References](#)[Tables](#)[Figures](#)[Back](#)[Close](#)[Full Screen / Esc](#)[Printer-friendly Version](#)[Interactive Discussion](#)

DC8 aircraft was based in Fairbanks, Alaska from 1st–21 April 2008 during ARCTAS-A and then in Cold Lake, Canada from 29 June–10 July 2008 during ARCTAS-B (Jacob et al., 2010). OH was measured by laser induced fluorescence aboard this flight, which has relatively high measurement uncertainties ($\pm 40\%$) (Brune et al., 1999). The POLARCAT-GRACE and POLARCAT-France projects had two aircraft jointly based in Kangerlussuaq, Greenland in summer. The POLARCAT-France ATR-42 measured CO using an infrared absorption analyser (Nédélec et al., 2003) and O_3 using an UV absorption instrument (Ancellet et al., 2009). The POLARCAT-GRACE Falcon also measured CO but used a vacuum UV fluorescence instrument (Gerbig et al., 1999) and O_3 was measured using a UV absorption analyser (Roiger et al., 2011). Even though based at the same location, the Falcon had a larger range than the ATR-42 and was able to cover larger regions and higher altitudes. The POLARCAT flight tracks are shown in Fig. 1.

4 Model evaluation

In this section, POLMIP model simulations are evaluated against Arctic surface CO and O_3 data and MOPITT CO retrievals throughout the year 2008. Aircraft measurements of CO, O_3 and OH from the POLARCAT and MOZAIC projects are then used to evaluate the vertical structure of the troposphere during intensive periods of sampling in April and June–July 2008. Model performance against the observations is summarised in Fig. 10 using the normalised mean gross error (NMGE), which gives the mean model bias (regardless of sign) over the vertical column or over the year as a percentage of the observed concentrations.

4.1 Seasonality of carbon monoxide and ozone

4.1.1 Arctic surface comparisons of carbon monoxide and ozone

Figure 2 shows the time series of monthly mean 2008 simulated and observed concentrations of CO at Barrow and Zeppelin and O₃ at Barrow and Summit (stations located north of the Arctic Circle). These models use the same emissions data, removing one key inter-model difference in Arctic surface CO and O₃ comparisons identified in Shindell et al. (2008). The overall model performance at several Arctic stations (shown in Fig. 1) is summarised as Taylor diagrams in Fig. 3. Perfect agreement between a model and observations would result in a normalised standard deviation (NSD) of 1, a correlation (*r*) of 1 and a centered root-mean-square difference (RMSD) of 0 (indicated by “Observed” on the Taylor diagram).

The models capture the seasonality in CO, with correlations greater than 0.8 at all surface stations. The models show a large range in their ability to capture the amplitude of the observed seasonal cycle ($0.3 \leq \text{NSD} \leq 1.2$). RMSDs are mostly clustered between values of 1 and 2. As this error statistic is weighted by monthly deviations from the annual mean, the models with a higher RMSD are the models which do not capture the amplitude of the seasonal cycle well. Figure 4 shows box and whisker plots of simulated seasonal mean surface CO bias at Barrow and Zeppelin. The median biases tend to lie below the zero line, showing that models generally underestimate CO throughout the year. However, the median biases are near zero in autumn, with some models overestimating CO in summer and autumn. The largest negative median biases occur during winter at Barrow and during spring at Zeppelin, with the smallest median biases occurring during autumn at both stations. This shows that state-of-the-art models still consistently underestimate winter/spring Arctic surface CO as shown in previous studies (e.g. Shindell et al., 2006, 2008).

Two models, GEOS-Chem and LMDZ-INCA, stand out from the other models in winter/spring, showing much better agreement with the observations due to higher simulated CO concentrations compared to other models. The version of the GEOS-Chem

**Chemical and
physical controls on
pollution transport to
the Arctic**

S. A. Monks et al.

Title Page

Abstract

Introduction

Conclusions

References

Tables

Figures



Back

Close

Full Screen / Esc

Printer-friendly Version

Interactive Discussion

in the Arctic and over the source regions ($r = 0.94$ – 0.99). At 300 hPa, a lower range in correlations ($r = 0.47$ – 0.98) indicates that the models are less able to capture the seasonal cycle at this altitude. As seen at the Arctic surface, most models underestimate CO at both levels throughout the year. The models which have the lowest/highest concentrations of CO throughout the year in the Arctic also have the lowest/highest concentrations near the source regions suggesting the individual model biases are consistent throughout the NH. The monthly model biases show a seasonal cycle (see bottom panel, Fig. 6), which is present across the different regions and models. At 700 hPa the largest regional biases tend to occur in winter and spring, as found at the Arctic surface stations, and the smallest biases occur in summer. However, at 300 hPa the bias shows the opposite behaviour, where the largest bias in all regions occurs in summer. This suggests that the surface winter/spring bias may be shifted to higher altitudes during summer when vertical mixing of pollutants by convection is important (e.g. Hov and Flatøy, 1997; Donnell et al., 2001; Jaegle, 2007).

Over North America the multi-model normalised mean gross error (NMGE, shown in Fig. 10) is smaller at 700 hPa relative to 300 hPa. Over Europe the NMGE is lower at 300 hPa relative to 700 hPa. The frequency of passing fronts, which export pollutants from the boundary layer to the free troposphere, are more frequent over North America compared to Europe (Stohl, 2001), which results in more rapid vertical transport of pollutants over North America (Wild and Akimoto, 2001). This may be shifting the negative model bias to a higher altitude to a larger extent than over Europe. However, over Asia, which also experiences very rapid vertical transport (Stohl, 2001), the NMGE is similar at 700 and 300 hPa. As can be seen in Fig. 6, there is no information available in the Arctic during winter and the mean DOFS over the Arctic region is much lower than in any other region, suggesting that there is limited information in the MOPITT retrieval in this region, making comparisons between the Arctic and the source regions difficult.

4.2 Vertical structure in the Arctic and Northern Hemisphere

4.2.1 POLARCAT Arctic aircraft comparisons

Aircraft measurements from the spring and summer 2008 POLARCAT campaign allow a detailed insight into model performance in the Arctic throughout the troposphere over regions of Greenland and the Canadian Arctic. The hourly gas-phase species from each model have been linearly interpolated in time and space to the location of the aircraft. The observed and simulated concentrations are separated into 50 hPa bins to give average vertical profiles over all flights. Aircraft profiles of CO, O₃, OH and water vapour for the DC8 spring and summer campaigns are shown in Fig. 7 and profiles of CO and O₃ for the POLARCAT-France and POLARCAT-GRACE summer campaigns are shown in Fig. 8.

ARCTAS-A spring comparisons

In April 2008, the CO and O₃ DC8 observations show a fairly homogeneous profile, with only small changes in concentrations from the surface up to the middle troposphere. Around 50 % of the CO measured came from anthropogenic sources in Asia, North America and Europe, with Asian emissions dominating (25 %) (Bian et al., 2013), most of which was emitted in China and India (Tilmes et al., 2011). Biomass burning emissions also contributed to the sampled CO, causing small enhancements in the observed profile (Bian et al., 2013; Tilmes et al., 2011) that can be seen at around 500 and 750 hPa in Fig. 7. Biomass burning also contributed a few ppbv to the sampled O₃ at the same levels (Wespes et al., 2012). In the upper troposphere, the influence of stratospheric mixing is at its greatest (Wespes et al., 2012), which can be seen by a large increase in O₃ and a concurrent decrease in CO.

The models capture the vertical structure well, yielding correlations of 0.96–0.99 for CO and 0.88–1.00 for O₃, however, only very small CO enhancements are seen in the simulated profiles at the altitude of the boreal fire plumes. This may be due to simulated

Chemical and physical controls on pollution transport to the Arctic

S. A. Monks et al.

Title Page

Abstract

Introduction

Conclusions

References

Tables

Figures



Back

Close

Full Screen / Esc

Printer-friendly Version

Interactive Discussion



Chemical and physical controls on pollution transport to the Arctic

S. A. Monks et al.

Title Page

Abstract

Introduction

Conclusions

References

Tables

Figures



Back

Close

Full Screen / Esc

Printer-friendly Version

Interactive Discussion



concentrations). The aircraft was ideally located to sample local fires that were burning in Canada at the time of the campaign, resulting in $\geq 60\%$ of the observed CO in the lower troposphere being directly emitted from boreal biomass burning (Bian et al., 2013). This can be seen in the observed profile in Fig. 7 as a large enhancement in CO at 900 hPa. Another enhancement in the observed CO profile is seen at 300 hPa, which is primarily due to the long-range transport of Asian anthropogenic and Siberian biomass burning emissions to Canada (Bian et al., 2013). O₃ shows a concurrent decrease in concentrations at 300 hPa and low O₃ near the surface, indicating O₃ production may have been limited within these plumes. In the lower troposphere, where fresh fire plumes were sampled, this is most likely due to the rapid conversion of NO_x to PAN, limiting O₃ production in the fire plumes (Alvarado et al., 2010). At 300 hPa, lower O₃ concentrations coincided with a limited influence from stratospheric O₃ relative to the surrounding air (Wespes et al., 2012), suggesting the sampling of air-masses that are not well-mixed with background air (Wespes et al., 2012).

Lower model-observed CO correlations ($r = 0.71\text{--}0.95$) show that the models agree less well with the observed CO vertical structure in the summer campaign compared to the spring, however, the main features of the profile are captured, with all models showing enhancements in CO at 300 and 900 hPa. Even though these enhancements are simulated by all models, the absolute concentrations vary widely, with some models having a high bias and some models having a low bias. In the middle troposphere, the models underestimate CO, as seen in spring, which suggests model background CO is still too low in summer in the middle troposphere. Global and regional models show similar overall performance, however the WRF-Chem 100 km resolution simulation has higher CO concentrations within the plume of enhanced CO at 900 hPa compared to the run at 50 km, suggesting model resolution has important impacts on concentrations near emission sources.

For O₃, the models show good agreement with the observed profile ($r = 0.78\text{--}0.99$). The models capture the decrease in O₃ seen at 300 hPa and the lower concentrations near the surface, however, as with CO, the models show a wide range in simulated O₃

Chemical and physical controls on pollution transport to the Arctic

S. A. Monks et al.

Title Page

Abstract

Introduction

Conclusions

References

Tables

Figures

◀

▶

◀

▶

Back

Close

Full Screen / Esc

Printer-friendly Version

Interactive Discussion



concentrations at 300 hPa. This may be related to the different chemical mechanisms in the models, which result in different O₃ production and loss efficiencies (Arnold et al., 2014). Summer OH correlations of 0.25–0.71 are lower than those calculated for the spring profile. In summer more rapid production and loss of OH leads to the observations being more sensitive to local changes in cloud cover, water vapour and O₃, making it even more difficult to simulate small spatial variability. Models show a wide spread in concentrations, however, they mostly lie within the 25th and 75th percentile of observed OH concentration. Model H₂O concentrations show good agreement with observations with the exception of a positive bias in the upper troposphere, as seen in spring. Model H₂O percent errors are slightly higher for most models in summer.

POLARCAT-France and POLARCAT-GRACE summer comparisons

As part of the summer POLARCAT campaign, the POLARCAT-France and POLARCAT-GRACE projects had two aircraft, the French ATR-42 and German DLR Falcon, based in Greenland during June–July 2008 to sample aged pollution transported to the Arctic (Law et al., 2014). For this reason, CO profiles sampled by these two aircraft (see Fig. 8) show lower concentrations compared to the DC8 summer measurements. They sampled a mixture of air types including background air, stratospheric air and plumes from anthropogenic and biomass burning sources that had been transported from North America, Asia and Europe (Law et al., 2014; Tilmes et al., 2011). Evidence of these polluted plumes can be seen in the ATR-42 CO profile at around 500 hPa and in the Falcon CO profile at 400 hPa. As seen during the ARCTAS-B campaign, there is a decrease in Falcon observed O₃ in these plumes relative to the surrounding air. Very little or no local emissions are indicated by CO concentrations that are lower than 100 ppbv being measured in the boundary layer.

As observed, modelled CO over Greenland is lower in comparison to concentrations simulated over the Canadian Arctic during the summer ARCTAS-B campaign. Most models underestimate the summer observed CO and show a large spread in simulated concentrations and their ability to capture the vertical structure ($r = 0.19$ – 0.91 for

monthly mean OH concentrations and the same transport (run as tracers within the TOMCAT CTM). It should be noted that whilst this will quantify the effect of transport and chemistry on inter-model differences in the idealised CO-like tracers, the results will not directly equate to the same inter-model differences in trace gases such as CO and O₃ due to other important factors, such as secondary CO production from other gases, such as CH₄ and NMHC. Firstly, it is useful to discuss model differences in OH and transport that will be studied using the idealised tracers.

5.1 Model differences in OH

Fig. 11 shows the annual zonal mean OH concentrations from each model, which are used to calculate loss rates for the OH-loss tracers. The primary route for OH production is by photolysis of O₃ in the presence of water vapour (Levy, 1971), with secondary production by recycling of HO₂ and H₂O₂, where the concentrations of NO_x and CO are important factors (Logan et al., 1981). The models simulate the highest concentrations of OH in the tropics, where the amount of incoming sunlight is at its greatest and O₃ is readily photolysed. Even though the models agree on this zonal distribution, the magnitude of OH and the location of the annual mean peak in OH vary. Due the importance of OH in controlling the lifetimes of most reactive trace gases in the atmosphere, these inter-model OH differences have important consequences for CO, both as its primary loss route and as a driver of secondary production from hydrocarbon oxidation.

Previous studies have related inter-model and intra-model changes in OH to variables which control its abundance. Voulgarakis et al. (2013) showed that present day global air-mass weighted OH concentrations from the Atmospheric Chemistry and Climate Model Intercomparison Project (ACCMIP) models were linearly related to model photolysis rates of O₃ to O(¹D) (JO(¹D)) and total volatile organic carbon (VOC) emissions. Murray et al. (2014) found that differences in the $S_N/S_C^{3/2}$ ratio, where S_N and S_C are the total sources of NO_x and of CO and hydrocarbons, respectively, together with

Chemical and physical controls on pollution transport to the Arctic

S. A. Monks et al.

Title Page

Abstract

Introduction

Conclusions

References

Tables

Figures



Back

Close

Full Screen / Esc

Printer-friendly Version

Interactive Discussion



the global tropospheric OH concentration, however, as OH controls the lifetime of CO it is not surprising to see such a correlation and it is unlikely to explain the spread in OH as the models use the same emission inventories.

Prinn et al. (2001) and Bousquet et al. (2005) estimated annual mean tropospheric air-mass weighted OH concentrations of $9.4 \pm 1.3 \times 10^5$ molec cm⁻³ and $9.8 \pm 1.3 \times 10^5$ molec cm⁻³, respectively, from the lifetime of the methyl chloroform. Eight POLMIP models simulate air-mass weighted global mean OH concentrations of 10.1 – 12.0×10^5 molec cm⁻³ (see Table S1 in the Supplement), with a multi-model mean of $10.8 \pm 0.6 \times 10^5$ molec cm⁻³, which is 10 % higher than the estimate of Bousquet et al. (2005). Bousquet et al. (2005) showed that OH was susceptible to inter-annual fluctuations in concentrations of around $8.5 \pm 1\%$. The POLMIP multi-model mean OH concentration lies slightly outside this range of inter-annual variability, suggesting OH in the POLMIP models may be slightly overestimated. For comparison, multi-model mean OH concentrations of $11.7 \pm 1.0 \times 10^5$ molec cm⁻³ (Voulgarakis et al., 2013) and $11.1 \pm 1.7 \times 10^5$ molec cm⁻³ (Shindell et al., 2006) have been found previously, suggesting OH is also slightly overestimated in other models, assuming estimates of OH from methyl chloroform are correct.

5.2 Model differences in tracer transport

Even though differences exist in the model OH, it is reasonable to expect that some of the model spread in CO is explained by differences in transport. Figure 13 shows the seasonal zonal mean difference between the sum of the simulated 25 day fixed loss regional tracer at two levels, 700 and 900 hPa. Negative values show there is more tracer in the upper 700 hPa level, positive values show that there is more tracer in the lower 900 hPa level and near zero values show a vertically well-mixed column (represented by the dashed line).

The largest positive values are found in the northern extra-tropics/lower mid-latitudes with very low CO differences in the Arctic and the tropics. In the Arctic, the models show near-zero differences in the winter and then negative differences in all other seasons. In

Chemical and physical controls on pollution transport to the Arctic

S. A. Monks et al.

Title Page

Abstract

Introduction

Conclusions

References

Tables

Figures



Back

Close

Full Screen / Esc

Printer-friendly Version

Interactive Discussion



Chemical and physical controls on pollution transport to the Arctic

S. A. Monks et al.

Title Page

Abstract

Introduction

Conclusions

References

Tables

Figures



Back

Close

Full Screen / Esc

Printer-friendly Version

Interactive Discussion



the highest concentrations of the 25 day fixed-loss tracer are located in the lowest altitude bin, with a clear decrease in absolute concentrations as altitude increases. This is in line with previous studies, which have shown poleward transport to occur mostly at low levels during winter (Klonecki et al., 2003; Stohl, 2006). As the year progresses, there is a clear shift in the concentrations to the higher altitude bins as transport of emissions at higher altitudes becomes more important in spring, summer and autumn (Klonecki et al., 2003).

Out of the three regional tracers, the European tracer shows the largest seasonal shift in transport efficiency to the Arctic. This is due to a large seasonal cycle in pollution export pathways from Europe (Duncan and Bey, 2004). The North American and Asian tracers show a much more consistent contribution to the Arctic total tracer concentration throughout the year and troposphere. Europe is the most important anthropogenic source region at the surface in winter, with Asian emissions dominating at the highest altitudes, which is consistent with the concept of the “polar dome”. Similar to Asia, the contribution from North America is larger at higher altitudes, although the magnitude is much smaller. This is most likely due to a combination of lower emissions and different export efficiencies (Stohl, 2006). These are in broad agreement with multi-model idealised tracer results from Shindell et al. (2008), despite differences in emissions, tracer lifetimes and the area of the regions used. Results at the surface and in the mid-troposphere also agree with idealised tracer experiments performed by Klonecki et al. (2003), but differ in the upper troposphere where they showed Asian emissions to have the smallest contribution and North American to have a much larger fractional contribution. Increases in Asian emissions (Ohara et al., 2007) and decreases in European and North American emissions since 1990 (Duncan and Logan, 2008), which will be important in terms of the relative contributions, will be accounted for in the Streets v1.2 emissions inventory used for the POLMIP simulations. Klonecki et al. (2003) used the EDGAR v2.0 CO emission estimates for the year 1990, explaining why the Asian influence is lower than North American in their study.

transport differ. This therefore suggests that differences in model emission inventories are the most likely cause of differences in the relative importance of anthropogenic emission regions in Arctic source contribution studies for the same chemical species (as found here for Asian emissions in the Arctic upper troposphere in comparison to Klonecki et al., 2003).

5.4 Inter-model variability in the Arctic

In this section, inter-model variability in CO and O₃ at Arctic surface stations is discussed whilst the possible causes of variability are explored with the use of the idealised tracers to compare the impact of inter-model differences in transport and OH.

5.4.1 Model variability in carbon monoxide and ozone

The interquartile range (IQR) of simulated CO and O₃ at selected Arctic stations are shown in Fig. 4 (Sect. 4.1.1), both as an absolute value (in ppbv) and as a percent (of the seasonal mean observed concentration). The IQR gives a measure of the amount of spread in the POLMIP models.

For CO, the largest model spread occurs during autumn, when the multi-model mean bias is at a minimum. The lowest model spread occurs during spring, when the multi-model mean bias is high. The magnitude of the IQR is relatively similar across the two stations, suggesting the cause of the model spread may equally affect CO throughout the Arctic. The IQR of modelled O₃ shows a large amount of spread during winter and spring and the lowest amount of model spread during summer. Model spread is larger at Barrow, suggesting that the causes of the model spread do not equally impact the different station locations. In addition, the seasonality in model spread differs between O₃ and CO, suggesting the underlying causes of model spread may depend on the trace gas considered.

Chemical and physical controls on pollution transport to the Arctic

S. A. Monks et al.

Title Page

Abstract

Introduction

Conclusions

References

Tables

Figures

◀

▶

◀

▶

Back

Close

Full Screen / Esc

Printer-friendly Version

Interactive Discussion



5.4.2 Model variability in OH and transport at Barrow

The 25 day fixed loss anthropogenic regional tracers are used to identify model differences in regional export to the Arctic surface and the OH loss anthropogenic regional tracers can be used as a proxy for differences in model chemistry that would result in different CO lifetimes and concentrations. Figure 16 shows seasonal box and whisker plots at Barrow for the fixed loss and OH loss tracers from eight of the POLMIP models. The interquartile range (IQR) of each sample is shown both as an absolute concentration and as a percentage of the multi-model mean concentration.

The IQR of the fixed loss tracers show that in winter the largest spread in model concentrations occurs in the European tracer. This coincides with the season when low-level export from Europe to the Arctic is particularly efficient (Duncan and Bey, 2004). This is shown by the winter European tracer having a higher median concentration than any other region and any other season (as expected from Sect. 5.3). In comparison to this, the model spread in the European tracer is relatively low throughout the rest of the year. The Asian tracer has the second largest wintertime spread compared to the other regional tracers, however, the largest overall spread in this tracer is seen in summer, with model spread also being relatively high in spring and autumn. The North American tracer shows very little spread throughout the year suggesting simulated transport from North America to Barrow is relatively similar between models. The large variability in the Asian tracer in summer and the European tracer in winter is likely to explain some of the model spread seen in the Arctic CO and O₃ concentrations at Barrow shown in Fig. 4. Better constraints on simulated wintertime transport from Europe and transport from Asia throughout the year may help to reduce model spread in CO and O₃ in the Arctic.

The IQR of the OH loss tracers shows that model spread is relatively consistent between the three different regions indicating that model OH differences affect all regions similarly, in contrast to inter-model transport differences. In terms of absolute concentrations, winter shows the largest overall spread in all three tracers. Spring and autumn

Chemical and physical controls on pollution transport to the Arctic

S. A. Monks et al.

Title Page

Abstract

Introduction

Conclusions

References

Tables

Figures



Back

Close

Full Screen / Esc

Printer-friendly Version

Interactive Discussion



differences are highly correlated with differences in model water vapour and photolysis rates, therefore improvements to these variables may reduce inter-model differences in Arctic trace species.

It is important to note that the results shown here are for idealised tracers and that the results may not be directly equated to simulations of CO and O₃, where complex chemistry plays a role. For example, if a model has higher OH than other models, then it is likely to have a faster CO loss rate and therefore lower CO concentrations, however, they will also have faster oxidation of methane and other hydrocarbons and therefore more secondary production of CO to offset the higher loss rate of CO. The extent that two opposing factors offset each other will be model dependent on differences in chemistry schemes. Shindell et al. (2008) concluded that oxidation rates, inferred from correlations between Arctic sensitivities and global CO lifetimes, did cause some inter-model differences in Arctic CO, but this was limited to the upper troposphere. The lack of any correlations in the lower troposphere is likely explained by the opposing impacts of OH on CO loss and secondary CO production, however, OH variability will still be particularly important in the when considering the production and loss terms of many reactive species in the Arctic.

6 Conclusions

We have used a range of surface, satellite and aircraft observations to evaluate multi-model simulations of CO and O₃ in the Arctic and sub-Arctic. The models include the same prescribed emissions for anthropogenic and biomass burning sources, removing one source of inter-model variability identified by previous model intercomparisons (Shindell et al., 2008), allowing the impacts of chemistry and transport differences on Arctic CO and O₃ burdens to be isolated.

The models broadly capture the observed seasonality of CO at the Arctic surface and over the mid-latitude lower troposphere. In agreement with previous studies, models generally underestimate CO in the Arctic at the surface, with the largest biases found

Chemical and physical controls on pollution transport to the Arctic

S. A. Monks et al.

Title Page

Abstract

Introduction

Conclusions

References

Tables

Figures



Back

Close

Full Screen / Esc

Printer-friendly Version

Interactive Discussion



correlations between CO and OH, the inter-model variability in the Arctic concentrations of OH-loss CO-like tracers is mostly driven by inter-model OH differences at lower latitudes, not OH differences in the Arctic.

We have investigated possible drivers of variability in mean tropospheric OH for a sub-set of POLMIP models. Mean tropospheric OH was found to be significantly correlated with mean tropospheric water vapour concentrations, both in the Arctic ($r^2 = 0.85$) and globally ($r^2 = 0.91$). This suggests better constraints on water vapour may reduce inter-model variability in global mean OH concentrations and therefore Arctic CO. Mean OH concentrations and $J(\text{O}^1\text{D})$ photolysis rates multiplied by O_3 concentrations were found to be significantly correlated within the Arctic ($r^2 = 0.65$), but not globally ($r^2 = 0.01$). This is not in agreement with results from the ACCMIP model intercomparison study, which found a significant correlation between present day OH and $J(\text{O}^1\text{D})$ in a group of chemistry-climate models (Voulgarakis et al., 2013). Some of the POLMIP models have similar chemical mechanisms which may be affecting these correlations and therefore a more detailed study of the causes of inter-model OH differences would be beneficial.

Whilst inter-model differences in transport and, most notably, OH are shown to be important in terms of the inter-model differences in the absolute concentrations of the CO-like tracers in the Arctic, the fractional contributions and, therefore, the relative importance of the different source regions (North America, Europe and Asia) and different source types (anthropogenic and biomass burning) are similar for both the fixed loss and OH-loss tracers. This suggests that differences in model emission inventories are the most likely cause of differences in the relative importance of different anthropogenic emission regions in Arctic source contribution studies for the same chemical species. In support of this, Klonecki et al. (2003), found Asian anthropogenic emissions to have the smallest fractional contribution in the Arctic upper troposphere using emission estimates based on the year 1990, whereas, in our analysis, using more recent emissions estimates, Asian emissions dominate. This illustrates the potential impact of increasing Asian emissions on the Arctic over the 20 year period since 1990. The

Chemical and physical controls on pollution transport to the Arctic

S. A. Monks et al.

Title Page

Abstract

Introduction

Conclusions

References

Tables

Figures

◀

▶

◀

▶

Back

Close

Full Screen / Esc

Printer-friendly Version

Interactive Discussion



anthropogenic emissions used for the POLMIP model simulations result in similar conclusions in terms of the relative importance of different anthropogenic source regions to emissions sensitivities (ppbv(CO) Tg⁻¹ emitted) to those reported by Shindell et al. (2008). Specifically, European emissions are most important at the surface in winter and Asian and North American emissions are most important at higher altitudes. In this study, emissions from fires in the boreal regions were also considered, and we showed that boreal fires can contribute 33, 43 and 19% to the total tracer in the Arctic in spring, summer and autumn, respectively, demonstrating the importance of fires as a source of Arctic pollution.

The Supplement related to this article is available online at doi:10.5194/acpd-14-25281-2014-supplement.

Acknowledgements. This work was supported by the EurEX project, funded by the UK Natural Environmental Research Council (ref: NE/H020241/1). S. A. Monks and S. R. Arnold acknowledge support from the European Commission via the FP7 EUFAR Integrating Activity. L. K. Emmons and S. Turquety acknowledge the National Center for Atmospheric Research, which is sponsored by the US National Science Foundation. Author L. K. Emmons acknowledges support from the National Aeronautics and Space Administration under award no. NNX08AD22G issued through the Science Mission Directorate, Tropospheric Composition Program. Authors (K. S. Law, G. Ancellet, J. L. Thomas, J.-C. Raut, S. Tilmes and Y. Long) acknowledge support from projects Agence National de Recherche (ANR) Climate Impact of Short-lived Climate Forcers and Methane in the Arctic (CLIMSLIP) Blanc SIMI 5–6 021 01 and CLIMSLIP-LEFE (CNRS-INSU). We acknowledge valuable help with WRF-Chem simulations from T. Onishi (LATMOS/IPSL) and G. Pfister (NCAR). J. Mao would like to acknowledge NOAA Climate Program Office grant NA13OAR4310071. We thank the POLARCAT aircraft teams, especially the NASA ARCTAS, DLR-GRACE, and French ATR-42 teams. French ATR-42 campaigns and data analysis were part of POLARCAT-France, funded by French Agence Nationale de la Recherche (ANR), CNES, CNRS-INSU-LEFE, IPEV and EUFAR. Thanks is given to all those involved in the collection and provision of data, specifically NOAA/ESRL/WDCGG for the surface data, the MOZAIC-IAGOS project for aircraft data and the MOPITT team for satellite data.

25319

ACPD

14, 25281–25350, 2014

Chemical and physical controls on pollution transport to the Arctic

S. A. Monks et al.

Title Page

Abstract

Introduction

Conclusions

References

Tables

Figures

⏪

⏩

◀

▶

Back

Close

Full Screen / Esc

Printer-friendly Version

Interactive Discussion



References

- ACIA: Arctic Climate Impact Assessment – Scientific Report, 21–60, Cambridge University Press, New York, USA, 2005. 25284
- Alvarado, M. J., Logan, J. A., Mao, J., Apel, E., Riemer, D., Blake, D., Cohen, R. C., Min, K.-E., Perring, A. E., Browne, E. C., Wooldridge, P. J., Diskin, G. S., Sachse, G. W., Fuelberg, H., Sessions, W. R., Harrigan, D. L., Huey, G., Liao, J., Case-Hanks, A., Jimenez, J. L., Cubison, M. J., Vay, S. A., Weinheimer, A. J., Knapp, D. J., Montzka, D. D., Flocke, F. M., Pollack, I. B., Wennberg, P. O., Kurten, A., Crounse, J., Clair, J. M. St., Wisthaler, A., Mikoviny, T., Yantosca, R. M., Carouge, C. C., and Le Sager, P.: Nitrogen oxides and PAN in plumes from boreal fires during ARCTAS-B and their impact on ozone: an integrated analysis of aircraft and satellite observations, *Atmos. Chem. Phys.*, 10, 9739–9760, doi:10.5194/acp-10-9739-2010, 2010. 25300
- Ancellet, G., Leclair de Bellevue, J., Mari, C., Nedelec, P., Kukui, A., Borbon, A., and Perros, P.: Effects of regional-scale and convective transports on tropospheric ozone chemistry revealed by aircraft observations during the wet season of the AMMA campaign, *Atmos. Chem. Phys.*, 9, 383–411, doi:10.5194/acp-9-383-2009, 2009. 25292
- Andersson, C., Langner, J., and Bergström, R.: Interannual variation and trends in air pollution over Europe due to climate variability during 1958–2001 simulated with a regional CTM coupled to the ERA40 reanalysis, *Tellus B*, 59, 77–98, 2007. 25333
- Archibald, A. T., Jenkin, M. E., and Shallcross, D. E.: An isoprene mechanism intercomparison, *Atmos. Environ.*, 44, 5356–5364, doi:10.1016/j.atmosenv.2009.09.016, Atmospheric Chemical Mechanisms: Selected Papers from the 2008 Conference, 2010. 25306
- Arnold, S. R., Emmons, L. K., Monks, S. A., Law, K. S., Ridley, D. A., Turquety, S., Tilmes, S., Thomas, J. L., Bouarar, I., Flemming, J., Huijnen, V., Mao, J., Duncan, B. N., Steenrod, S., Yoshida, Y., Langner, J., and Long, Y.: Biomass burning influence on high latitude tropospheric ozone and reactive nitrogen in summer 2008: a multi-model analysis based on POLMIP simulations, *Atmos. Chem. Phys. Discuss.*, 14, 24573–24621, doi:10.5194/acpd-14-24573-2014, 2014. 25301
- Atlas, E. L., Ridley, B. A., and Cantrell, C.: The Tropospheric Ozone Production about the Spring Equinox (TOPSE) Experiment: Introduction, *J. Geophys. Res.*, 108, 8353, doi:10.1029/2002JD003172, 2003. 25285

Chemical and physical controls on pollution transport to the Arctic

S. A. Monks et al.

Title Page

Abstract

Introduction

Conclusions

References

Tables

Figures



Back

Close

Full Screen / Esc

Printer-friendly Version

Interactive Discussion



**Chemical and
physical controls on
pollution transport to
the Arctic**

S. A. Monks et al.

Title Page

Abstract

Introduction

Conclusions

References

Tables

Figures



Back

Close

Full Screen / Esc

Printer-friendly Version

Interactive Discussion



Duncan, B. N., Strahan, S. E., Yoshida, Y., Steenrod, S. D., and Livesey, N.: Model study of the cross-tropopause transport of biomass burning pollution, *Atmos. Chem. Phys.*, 7, 3713–3736, doi:10.5194/acp-7-3713-2007, 2007. 25333

Eckhardt, S., Stohl, A., Wernli, H., James, P., Forster, C., and Spichtinger, N.: A 15-year climatology of warm conveyor belts, *J. Climate*, 17, 218–237, 2004. 25286

Emmons, L. K., Walters, S., Hess, P. G., Lamarque, J.-F., Pfister, G. G., Fillmore, D., Granier, C., Guenther, A., Kinnison, D., Laepple, T., Orlando, J., Tie, X., Tyndall, G., Wiedinmyer, C., Baughcum, S. L., and Kloster, S.: Description and evaluation of the Model for Ozone and Related chemical Tracers, version 4 (MOZART-4), *Geosci. Model Dev.*, 3, 43–67, doi:10.5194/gmd-3-43-2010, 2010. 25333

Emmons, L., Arnold, S. R., Monks, S., Huijnen, V., Tilmes, S., Law, K., Turquety, S., Long, Y., Thomas, J., Bouarar, I., Duncan, B., Steenrod, S., Strode, S., Flemming, J., Mao, J., and Langner, J.: The POLARCAT Model Intercomparison Project (POLMIP): overview and evaluation with observations, *Atmos. Chem. Phys. Discuss.*, in preparation, 2014. 25288, 25289, 25290

Fast, J. D., Gustafson, W. I., Easter, R. C., Zaveri, R. A., Barnard, J. C., Chapman, E. G., Grell, G. A., and Peckham, S. E.: Evolution of ozone, particulates, and aerosol direct radiative forcing in the vicinity of Houston using a fully coupled meteorology-chemistry-aerosol model, *J. Geophys. Res.-Atmos.*, 111, D21305, doi:10.1029/2005JD006721, 2006. 25333

Fisher, J. A., Jacob, D. J., Purdy, M. T., Kopacz, M., Le Sager, P., Carouge, C., Holmes, C. D., Yantosca, R. M., Batchelor, R. L., Strong, K., Diskin, G. S., Fuelberg, H. E., Holloway, J. S., Hyer, E. J., McMillan, W. W., Warner, J., Streets, D. G., Zhang, Q., Wang, Y., and Wu, S.: Source attribution and interannual variability of Arctic pollution in spring constrained by aircraft (ARCTAS, ARCPAC) and satellite (AIRS) observations of carbon monoxide, *Atmos. Chem. Phys.*, 10, 977–996, doi:10.5194/acp-10-977-2010, 2010. 25285

Flemming, J., Huijnen, V., Jones, L., Arteta, J., and Massart, S.: Technical Documentations of C-IFS (On-line integration of atmospheric chemistry in the Integrated Forecasting System), available at: http://www.gmes-atmosphere.eu/documents/deliverables/g-rg/G-RG_4.8.pdf (last access: 25 September 2014), 2012. 25333

Fuelberg, H. E., Harrigan, D. L., and Sessions, W.: A meteorological overview of the ARCTAS 2008 mission, *Atmos. Chem. Phys.*, 10, 817–842, doi:10.5194/acp-10-817-2010, 2010. 25296

Chemical and physical controls on pollution transport to the Arctic

S. A. Monks et al.

Title Page

Abstract

Introduction

Conclusions

References

Tables

Figures



Back

Close

Full Screen / Esc

Printer-friendly Version

Interactive Discussion



Gerbig, C., Schmitgen, S., Kley, D., Volz-Thomas, A., Dewey, K., and Haaks, D.: An improved fast-response vacuum-UV resonance fluorescence CO instrument, *J. Geophys. Res.*, 104, 1699–1704, 1999. 25292

5 Grell, G. A., Peckham, S. E., Schmitz, R., McKeen, S. A., Frost, G., Skamarock, W. C., and Eder, B.: Fully coupled ‘online’ chemistry within the WRF model, *Atmos. Environ.*, 39, 6957–6975, doi:10.1016/j.atmosenv.2005.04.027, 2005. 25333

10 Guenther, A. B., Jiang, X., Heald, C. L., Sakulyanontvittaya, T., Duhl, T., Emmons, L. K., and Wang, X.: The Model of Emissions of Gases and Aerosols from Nature version 2.1 (MEGAN2.1): an extended and updated framework for modeling biogenic emissions, *Geosci. Model Dev.*, 5, 1471–1492, doi:10.5194/gmd-5-1471-2012, 2012. 25289

Harriss, R. C., Wofsy, S. C., Hoell, J. M., J., Bendura, R. J., Drewry, J. W., McNeal, R. J., Pierce, D., Rabine, V., and Snell, R. L.: The Arctic Boundary Layer Expedition (ABLE-3B): July–August 1990, *J. Geophys. Res.*, 99, 1635–1643, 1994. 25287

15 Helmig, D., Oltmans, S. J., Carlson, D., Lamarque, J.-F., Jones, A., Labuschagne, C., Anlauf, K., and Hayden, K.: A review of surface ozone in the polar regions, *Atmos. Environ.*, 41, 5138–5161, 2007. 25286, 25294, 25295

Helmig, D., Cohen, L. D., Bocquet, F., Oltmans, S., Grachev, A., and Neff, W.: Spring and summertime diurnal surface ozone fluxes over the polar snow at Summit, Greenland, *Geophys. Res. Lett.*, 36, L08809, doi:10.1029/2008GL036549, 2009. 25302

20 Hirdman, D., Sodemann, H., Eckhardt, S., Burkhardt, J. F., Jefferson, A., Mefford, T., Quinn, P. K., Sharma, S., Ström, J., and Stohl, A.: Source identification of short-lived air pollutants in the Arctic using statistical analysis of measurement data and particle dispersion model output, *Atmos. Chem. Phys.*, 10, 669–693, doi:10.5194/acp-10-669-2010, 2010. 25285, 25295

25 Hourdin, F., Musat, I., Bony, S., Braconnot, P., Codron, F., Dufresne, J.-L., Fairhead, L., Filiberti, M.-A., Friedlingstein, P., Grandpeix, J.-Y., Krinner, G., LeVan, P., Li, Z.-X., and Lott, F.: The LMDZ4 general circulation model: climate performance and sensitivity to parametrized physics with emphasis on tropical convection, *Clim. Dynam.*, 27, 787–813, doi:10.1007/s00382-006-0158-0, 2006. 25333

30 Hov, Ø., and Flatøy, F.: Convective redistribution of ozone and oxides of nitrogen in the troposphere over Europe in summer and fall, *J. Atmos. Chem.*, 28, 319–337, doi:10.1023/A:1005780730600, 1997. 25297

Huijnen, V., Williams, J., van Weele, M., van Noije, T., Krol, M., Dentener, F., Segers, A., Houweling, S., Peters, W., de Laat, J., Boersma, F., Bergamaschi, P., van Velthoven, P., Le Sager, P.,

**Chemical and
physical controls on
pollution transport to
the Arctic**

S. A. Monks et al.

Title Page

Abstract

Introduction

Conclusions

References

Tables

Figures



Back

Close

Full Screen / Esc

Printer-friendly Version

Interactive Discussion

Eskes, H., Alkemade, F., Scheele, R., Nédélec, P., and Pätz, H.-W.: The global chemistry transport model TM5: description and evaluation of the tropospheric chemistry version 3.0, *Geosci. Model Dev.*, 3, 445–473, doi:10.5194/gmd-3-445-2010, 2010. 25333

Iversen, T.: Numerical modelling of the long range atmospheric transport of sulphur dioxide and particulate sulphate to the arctic, *Atmos. Environ.* (1967), 23, 2571–2595, doi:10.1016/0004-6981(89)90267-9, 1989. 25285

Jacob, D. J., Crawford, J. H., Maring, H., Clarke, A. D., Dibb, J. E., Emmons, L. K., Ferrare, R. A., Hostetler, C. A., Russell, P. B., Singh, H. B., Thompson, A. M., Shaw, G. E., McCauley, E., Pederson, J. R., and Fisher, J. A.: The Arctic Research of the Composition of the Troposphere from Aircraft and Satellites (ARCTAS) mission: design, execution, and first results, *Atmos. Chem. Phys.*, 10, 5191–5212, doi:10.5194/acp-10-5191-2010, 2010. 25292

Jaegle, L.: Pumping up surface air, *Science*, 315, 772–773, doi:10.1126/science.1138988, 2007. 25297

Khalil, M. A. K. and Rasmussen, R. A.: Statistical analysis of trace gases in Arctic haze, *Geophys. Res. Lett.*, 11, 437–440, 1984. 25285

Khalil, M. A. K., and Rasmussen, R. A.: Global decrease in atmospheric carbon monoxide concentration, *Nature*, 370, 639–641, 1994. 25287

Klonecki, A., Hess, P., Emmons, L., Smith, L., Orlando, J., and Blake, D.: Seasonal changes in the transport of pollutants into the Arctic troposphere—model study, *J. Geophys. Res.*, 108, 8367, doi:10.1029/2001JD001390, 2003. 25285, 25286, 25288, 25309, 25311, 25318

Koch, D. and Hansen, J.: Distant origins of Arctic black carbon: a Goddard institute for space studies modell experiment, *J. Geophys. Res.*, 110, D04204, doi:10.1029/2004JD005296, 2005. 25285

Kopacz, M., Jacob, D. J., Fisher, J. A., Logan, J. A., Zhang, L., Megretskaia, I. A., Yantosca, R. M., Singh, K., Henze, D. K., Burrows, J. P., Buchwitz, M., Khlystova, I., McMillan, W. W., Gille, J. C., Edwards, D. P., Eldering, A., Thouret, V., and Nedelec, P.: Global estimates of CO sources with high resolution by adjoint inversion of multiple satellite datasets (MOPITT, AIRS, SCIAMACHY, TES), *Atmos. Chem. Phys.*, 10, 855–876, doi:10.5194/acp-10-855-2010, 2010. 25287, 25315

Lamarque, J.-F., Emmons, L. K., Hess, P. G., Kinnison, D. E., Tilmes, S., Vitt, F., Heald, C. L., Holland, E. A., Lauritzen, P. H., Neu, J., Orlando, J. J., Rasch, P. J., and Tyndall, G. K.: CAM-chem: description and evaluation of interactive atmospheric chemistry in the Community

Chemical and physical controls on pollution transport to the Arctic

S. A. Monks et al.

Title Page

Abstract

Introduction

Conclusions

References

Tables

Figures



Back

Close

Full Screen / Esc

Printer-friendly Version

Interactive Discussion



Earth System Model, *Geosci. Model Dev.*, 5, 369–411, doi:10.5194/gmd-5-369-2012, 2012. 25333

Law, K. S. and Stohl, A.: Arctic air pollution: origins and impacts, *Science*, 315, 1537–1540, doi:10.1126/science.1137695, 2007. 25308

5 Law, K., Stohl, A., Quinn, P., Brock, C., Burkhardt, J., Paris, J., Ancellet, G., Singh, H., Roiger, A., Schlager, H., Dibb, J., Jacob, D., Arnold, S., Pelon, J., and Thomas, J.: Arctic air pollution: new insights from POLARCAT-IPY, *B. Am. Meteorol. Soc.*, doi:10.1175/BAMS-D-13-00017.1, in press, 2014. 25288, 25291, 25295, 25296, 25301, 25308, 25310

10 Lawrence, M. G., Jöckel, P., and von Kuhlmann, R.: What does the global mean OH concentration tell us?, *Atmos. Chem. Phys.*, 1, 37–49, doi:10.5194/acp-1-37-2001, 2001. 25345

Legrand, M., De Angelis, M., Staffelbach, T., Neftel, A., and Stauffer, B.: Large perturbations of ammonium and organic acids content in the summit Greenland Ice Core. Fingerprint from forest fires?, *Geophys. Res. Lett.*, 19, 473–475, 1992. 25287

15 Levy, H.: Normal atmosphere: large radical and formaldehyde concentrations predicted, *Science*, 173, 141–143, doi:10.1126/science.173.3992.141, 1971. 25305

Logan, J. A., Prather, M. J., Wofsy, S. C., and McElroy, M. B.: Tropospheric chemistry: a global perspective, *J. Geophys. Res.-Oceans*, 86, 7210–7254, doi:10.1029/JC086iC08p07210, 1981. 25305

20 Macintyre, H. L. and Evans, M. J.: Parameterisation and impact of aerosol uptake of HO₂ on a global tropospheric model, *Atmos. Chem. Phys. Discuss.*, 11, 16311–16334, doi:10.5194/acpd-11-16311-2011, 2011. 25316

25 Mao, J., Jacob, D. J., Evans, M. J., Olson, J. R., Ren, X., Brune, W. H., Clair, J. M. St., Crouse, J. D., Spencer, K. M., Beaver, M. R., Wennberg, P. O., Cubison, M. J., Jimenez, J. L., Fried, A., Weibring, P., Walega, J. G., Hall, S. R., Weinheimer, A. J., Cohen, R. C., Chen, G., Crawford, J. H., McNaughton, C., Clarke, A. D., Jaeglé, L., Fisher, J. A., Yantosca, R. M., Le Sager, P., and Carouge, C.: Chemistry of hydrogen oxide radicals (HO_x) in the Arctic troposphere in spring, *Atmos. Chem. Phys.*, 10, 5823–5838, doi:10.5194/acp-10-5823-2010, 2010. 25333

30 Mao, J., Fan, S., Jacob, D. J., and Travis, K. R.: Radical loss in the atmosphere from Cu-Fe redox coupling in aerosols, *Atmos. Chem. Phys.*, 13, 509–519, doi:10.5194/acp-13-509-2013, 2013. 25287, 25294, 25315

Monks, S. A.: A model study of chemistry and transport in the Arctic troposphere, Ph. D. thesis, University of Leeds, 2011. 25333

**Chemical and
physical controls on
pollution transport to
the Arctic**

S. A. Monks et al.

Title Page

Abstract

Introduction

Conclusions

References

Tables

Figures



Back

Close

Full Screen / Esc

Printer-friendly Version

Interactive Discussion



Monks, S. A., Arnold, S. R., and Chipperfield, M. P.: Evidence for El Niño–Southern Oscillation (ENSO) influence on Arctic CO interannual variability through biomass burning emissions, *Geophys. Res. Lett.*, 39, L14804, doi:10.1029/2012GL052512, 2012. 25287, 25310

Murray, L. T., Mickley, L. J., Kaplan, J. O., Sofen, E. D., Pfeiffer, M., and Alexander, B.: Factors controlling variability in the oxidative capacity of the troposphere since the Last Glacial Maximum, *Atmos. Chem. Phys.*, 14, 3589–3622, doi:10.5194/acp-14-3589-2014, 2014. 25305

Nedelec, P., Cammas, J.-P., Thouret, V., Athier, G., Cousin, J.-M., Legrand, C., Abonne, C., Lecoq, F., Cayez, G., and Marizy, C.: An improved infrared carbon monoxide analyser for routine measurements aboard commercial Airbus aircraft: technical validation and first scientific results of the MOZAIC III programme, *Atmos. Chem. Phys.*, 3, 1551–1564, doi:10.5194/acp-3-1551-2003, 2003. 25291, 25292

Novelli, P. C., Masarie, K. A., Tans, P. P., and Lang, P. M.: Recent changes in atmospheric carbon monoxide, *Science*, 263, 1587–1590, doi:10.1126/science.263.5153.1587, 1994. 25287

Novelli, P., Masarie, K., and Lang, P.: Distributions and recent changes of carbon monoxide in the lower troposphere, *J. Geophys. Res.*, 103, 19015–19033, 1998. 25290

Ohara, T., Akimoto, H., Kurokawa, J., Horii, N., Yamaji, K., Yan, X., and Hayasaka, T.: An Asian emission inventory of anthropogenic emission sources for the period 1980–2020, *Atmos. Chem. Phys.*, 7, 4419–4444, doi:10.5194/acp-7-4419-2007, 2007. 25287, 25309

Oltmans, S. J. and Levy, H.: Surface ozone measurements from a global network, *Atmos. Environ.*, 28, 9–24, doi:10.1016/1352-2310(94)90019-1, 1994. 25290

Oltmans, S., Lefohn, A., Harris, J., Galbally, I., Scheel, H., Bodeker, G., Brunke, E., Claude, H., Tarasick, D., Johnson, B., Simmonds, P., Shadwick, D., Anlauf, K., Hayden, K., Schmidlin, F., Fujimoto, T., Akagi, K., Meyer, C., Nichol, S., Davies, J., Redondas, A., and Cuevas, E.: Long-term changes in tropospheric ozone, *Atmos. Environ.*, 40, 3156–3173, doi:10.1016/j.atmosenv.2006.01.029, 2006. 25286

Oltmans, S. J., Lefohn, A. S., Scheel, H. E., Harris, J. M., Levy, H. I., Galbally, I. E., Brunke, E., Meyer, C. P., Lathrop, J. A., Johnson, B. J., Shadwick, D. S., Cuevas, E., Schmidlin, F. J., Tarasick, D. W., Claude, H., Kerr, J. B., Uchino, O., and Mohnen, V.: Trends of ozone in the troposphere, *Geophys. Res. Lett.*, 25, 139–142, 1998. 25286

Paris, J.-D., Stohl, A., Nédélec, P., Arshinov, M. Yu., Panchenko, M. V., Shmargunov, V. P., Law, K. S., Belan, B. D., and Ciais, P.: Wildfire smoke in the Siberian Arctic in summer: source characterization and plume evolution from airborne measurements, *Atmos. Chem. Phys.*, 9, 9315–9327, doi:10.5194/acp-9-9315-2009, 2009. 25287

Chemical and physical controls on pollution transport to the Arctic

S. A. Monks et al.

Title Page

Abstract

Introduction

Conclusions

References

Tables

Figures



Back

Close

Full Screen / Esc

Printer-friendly Version

Interactive Discussion



- Parrella, J. P., Jacob, D. J., Liang, Q., Zhang, Y., Mickley, L. J., Miller, B., Evans, M. J., Yang, X., Pyle, J. A., Theys, N., and Van Roozendael, M.: Tropospheric bromine chemistry: implications for present and pre-industrial ozone and mercury, *Atmos. Chem. Phys.*, 12, 6723–6740, doi:10.5194/acp-12-6723-2012, 2012. 25333
- 5 Pommier, M., Law, K. S., Clerbaux, C., Turquety, S., Hurtmans, D., Hadji-Lazaro, J., Coheur, P.-F., Schlager, H., Ancellet, G., Paris, J.-D., Nédélec, P., Diskin, G. S., Podolske, J. R., Holloway, J. S., and Bernath, P.: IASI carbon monoxide validation over the Arctic during POLARCAT spring and summer campaigns, *Atmos. Chem. Phys.*, 10, 10655–10678, doi:10.5194/acp-10-10655-2010, 2010. 25296
- 10 Prinn, R. G., Huang, J., Weiss, R. F., Cunnold, D. M., Fraser, P. J., Simmonds, P. G., McCulloch, A., Harth, C., Salameh, P., O'Doherty, S., Wang, R. H. J., Porter, L., and Miller, B. R.: Evidence for substantial variations of atmospheric hydroxyl radicals in the past two decades, *Science*, 292, 1882–1888, 2001. 25307, 25315
- 15 Quinn, P. K., Bates, T. S., Baum, E., Doubleday, N., Fiore, A. M., Flanner, M., Fridlind, A., Garrett, T. J., Koch, D., Menon, S., Shindell, D., Stohl, A., and Warren, S. G.: Short-lived pollutants in the Arctic: their climate impact and possible mitigation strategies, *Atmos. Chem. Phys.*, 8, 1723–1735, doi:10.5194/acp-8-1723-2008, 2008. 25284
- Rahn, K. A.: Progress in Arctic air chemistry, 1980–1984, *Atmos. Environ. (1967)*, 19, 1987–1994, doi:10.1016/0004-6981(85)90107-6, 1985. 25285
- 20 Randerson, J. T., Liu, H., Flanner, M. G., Chambers, S. D., Jin, Y., Hess, P. G., Pfister, G., Mack, M. C., Treseder, K. K., Welp, L. R., Chapin, F. S., Harden, J. W., Goulden, M. L., Lyons, E., Neff, J. C., Schuur, E. A. G., and Zender, C. S.: The impact of boreal forest fire on climate warming, *Science*, 314, 1130–1132, doi:10.1126/science.1132075, 2006. 25287
- Robertson, L., Langner, J., and Engardt, M.: An Eulerian limited area atmospheric transport model, *J. Appl. Meteorol.*, 38, 90–210, 1999. 25333
- 25 Roiger, A., Schlager, H., Schäfler, A., Huntrieser, H., Scheibe, M., Aufmhoff, H., Cooper, O. R., Sodemann, H., Stohl, A., Burkhardt, J., Lazzara, M., Schiller, C., Law, K. S., and Arnold, F.: In-situ observation of Asian pollution transported into the Arctic lowermost stratosphere, *Atmos. Chem. Phys.*, 11, 10975–10994, doi:10.5194/acp-11-10975-2011, 2011. 25292, 25302
- 30 Schnell, R. C. and Raatz, W. E.: Vertical and horizontal characteristics of Arctic haze during AGASP: Alaskan Arctic, *Geophys. Res. Lett.*, 11, 369–372, 1984. 25285
- Schnell, R. C., Watson, T. B., and Bodhaine, B. A.: NOAA WP-3D instrumentation and flight operations on AGASP-II, *J. Atmos. Chem.*, 9, 3–16, doi:10.1007/BF00052822, 1989. 25285

Chemical and physical controls on pollution transport to the Arctic

S. A. Monks et al.

Title Page

Abstract

Introduction

Conclusions

References

Tables

Figures



Back

Close

Full Screen / Esc

Printer-friendly Version

Interactive Discussion



- Serreze, M. C. and Francis, J. A.: The Arctic amplification debate, *Climatic Change*, 76, 241–264, 2006. 25284
- Shaw, G. E.: The Arctic haze phenomenon, *B. Am. Meteorol. Soc.*, 76, 2403–2413, 1995. 25285
- 5 Shindell, D.: Local and remote contributions to Arctic warming, *Geophys. Res. Lett.*, 34, L14704, doi:10.1029/2007GL030221, 2007. 25284
- Shindell, D. and Faluvegi, G.: Climate response to regional radiative forcing during the twentieth century, *Nat. Geosci.*, 2, 294–300, 2009. 25284
- Shindell, D. T., Faluvegi, G., Stevenson, D. S., Krol, M. C., Emmons, L. K., Lamarque, J.-F.,
10 Pétron, G., Dentener, F. J., Ellingsen, K., Schultz, M. G., Wild, O., Amann, M., Atherton, C. S.,
Bergmann, D. J., Bey, I., Butler, T., Cofala, J., Collins, W. J., Derwent, R. G., Doherty, R. M.,
Drevet, J., Eskes, H. J., Fiore, A. M., Gauss, M., Hauglustaine, D. A., Horowitz, L. W., Isak-
sen, I. S. A., Lawrence, M. G., Montanaro, V., Müller, J.-F., Pitari, G., Prather, M. J., Pyle, J. A.,
Rast, S., Rodriguez, J. M., Sanderson, M. G., Savage, N. H., Strahan, S. E., Sudo, K.,
15 Szopa, S., Unger, N., van Noije, T. P. C., and Zeng, G.: Multimodel simulations of carbon
monoxide: comparison with observations and projected near-future changes, *J. Geophys.
Res.*, 111, D19306, doi:10.1029/2006JD007100, 2006. 25287, 25293, 25296, 25307
- Shindell, D. T., Chin, M., Dentener, F., Doherty, R. M., Faluvegi, G., Fiore, A. M., Hess, P.,
Koch, D. M., MacKenzie, I. A., Sanderson, M. G., Schultz, M. G., Schulz, M., Steven-
20 son, D. S., Teich, H., Textor, C., Wild, O., Bergmann, D. J., Bey, I., Bian, H., Cuvelier, C., Dun-
can, B. N., Folberth, G., Horowitz, L. W., Jonson, J., Kaminski, J. W., Marmer, E., Park, R.,
Pringle, K. J., Schroeder, S., Szopa, S., Takemura, T., Zeng, G., Keating, T. J., and Zuber, A.:
A multi-model assessment of pollution transport to the Arctic, *Atmos. Chem. Phys.*, 8, 5353–
5372, doi:10.5194/acp-8-5353-2008, 2008. 25286, 25287, 25293, 25294, 25295, 25309,
25 25314, 25317, 25319
- Sodemann, H., Pommier, M., Arnold, S. R., Monks, S. A., Stebel, K., Burkhardt, J. F., Hair, J. W.,
Diskin, G. S., Clerbaux, C., Coheur, P.-F., Hurtmans, D., Schlager, H., Blechschmidt, A.-M.,
Kristjánsson, J. E., and Stohl, A.: Episodes of cross-polar transport in the Arctic troposphere
during July 2008 as seen from models, satellite, and aircraft observations, *Atmos. Chem.
30 Phys.*, 11, 3631–3651, doi:10.5194/acp-11-3631-2011, 2011. 25285, 25302
- Solberg, S., Dye, C., Schmidbauer, N., Herzog, A., and Gehrig, R.: Carbonyls and nonmethane
hydrocarbons at rural European sites from the mediterranean to the arctic, *J. Atmos. Chem.*,
25, 33–66, doi:10.1007/BF00053285, 1996. 25285

**Chemical and
physical controls on
pollution transport to
the Arctic**

S. A. Monks et al.

Title Page

Abstract

Introduction

Conclusions

References

Tables

Figures



Back

Close

Full Screen / Esc

Printer-friendly Version

Interactive Discussion



- Stohl, A.: A 1-year Lagrangian climatology of airstreams in the Northern Hemisphere troposphere and lowermost stratosphere, *J. Geophys. Res.*, 106, 7263–7279, 2001. 25286, 25297
- Stohl, A.: Characteristics of atmospheric transport into the Arctic troposphere, *J. Geophys. Res.*, 111, D11306, doi:10.1029/2005JD006888, 2006. 25285, 25286, 25308, 25309
- 5 Strahan, S. E., Duncan, B. N., and Hoor, P.: Observationally derived transport diagnostics for the lowermost stratosphere and their application to the GMI chemistry and transport model, *Atmos. Chem. Phys.*, 7, 2435–2445, doi:10.5194/acp-7-2435-2007, 2007. 25333
- Szopa, S., Balkanski, Y., Schulz, M., Bekki, S., Cugnet, D., Fortems-Cheiney, A., Turquety, S., Cozic, A., Déandreis, C., Hauglustaine, D., Idelkadi, A., Lathièrre, J., Lefevre, F.,
10 Marchand, M., Vuolo, R., Yan, N., and Dufresne, J.-L.: Aerosol and ozone changes as forcing for climate evolution between 1850 and 2100, *Clim. Dynam.*, 40, 2223–2250, doi:10.1007/s00382-012-1408-y, 2013. 25333
- Thomas, J. L., Raut, J.-C., Law, K. S., Marelle, L., Ancellet, G., Ravetta, F., Fast, J. D., Pfister, G., Emmons, L. K., Diskin, G. S., Weinheimer, A., Roiger, A., and Schlager, H.: Pollution transport from North America to Greenland during summer 2008, *Atmos. Chem. Phys.*, 13, 3825–3848, doi:10.5194/acp-13-3825-2013, 2013. 25287, 25302
- 15 Thouret, V., Marengo, A., Logan, J. A., Nédélec, P., and Grouhel, C.: Comparisons of ozone measurements from the MOZAIC airborne program and the ozone sounding network at eight locations, *J. Geophys. Res.-Atmos.*, 103, 25695–25720, doi:10.1029/98JD02243, 1998. 25291
- 20 Tilmes, S., Emmons, L. K., Law, K. S., Ancellet, G., Schlager, H., Paris, J.-D., Fuelberg, H. E., Streets, D. G., Wiedinmyer, C., Diskin, G. S., Kondo, Y., Holloway, J., Schwarz, J. P., Spackman, J. R., Campos, T., Nédélec, P., and Panchenko, M. V.: Source contributions to Northern Hemisphere CO and black carbon during spring and summer 2008 from POLARCAT and START08/preHIPPO observations and MOZART-4, *Atmos. Chem. Phys. Discuss.*, 11, 5935–5983, doi:10.5194/acpd-11-5935-2011, 2011. 25287, 25298, 25301, 25302
- 25 Voulgarakis, A., Naik, V., Lamarque, J.-F., Shindell, D. T., Young, P. J., Prather, M. J., Wild, O., Field, R. D., Bergmann, D., Cameron-Smith, P., Cionni, I., Collins, W. J., Dalsøren, S. B., Doherty, R. M., Eyring, V., Faluvegi, G., Folberth, G. A., Horowitz, L. W., Josse, B., MacKenzie, I. A., Nagashima, T., Plummer, D. A., Righi, M., Rumbold, S. T., Stevenson, D. S., Strode, S. A., Sudo, K., Szopa, S., and Zeng, G.: Analysis of present day and future OH and methane lifetime in the ACCMIP simulations, *Atmos. Chem. Phys.*, 13, 2563–2587, doi:10.5194/acp-13-2563-2013, 2013. 25305, 25306, 25307, 25318
- 30

**Chemical and
physical controls on
pollution transport to
the Arctic**

S. A. Monks et al.

Title Page

Abstract

Introduction

Conclusions

References

Tables

Figures



Back

Close

Full Screen / Esc

Printer-friendly Version

Interactive Discussion

- Walker, T. W., Jones, D. B. A., Parrington, M., Henze, D. K., Murray, L. T., Bottenheim, J. W., Anlauf, K., Worden, J. R., Bowman, K. W., Shim, C., Singh, K., Kopacz, M., Tarasick, D. W., Davies, J., von der Gathen, P., Thompson, A. M., and Carouge, C. C.: Impacts of midlatitude precursor emissions and local photochemistry on ozone abundances in the Arctic, *J. Geophys. Res.-Atmos.*, 117, D01305, doi:10.1029/2011JD016370, 2012. 25285
- 5 Warneke, C., Bahreini, R., Brioude, J., Brock, C. A., de Gouw, J. A., Fahey, D. W., Froyd, K. D., Holloway, J. S., Middlebrook, A., Miller, L., Montzka, S., Murphy, D. M., Peischl, J., Ryerson, T. B., Schwarz, J. P., Spackman, J. R., and Veres, P.: Biomass burning in Siberia and Kazakhstan as an important source for haze over the Alaskan Arctic in April 2008, *Geophys. Res. Lett.*, 36, L02813, doi:10.1029/2008GL036194, 2009. 25295
- 10 Warneke, C., Froyd, K. D., Brioude, J., Bahreini, R., Brock, C. A., Cozic, J., de Gouw, J. A., Fahey, D. W., Ferrare, R., Holloway, J. S., Middlebrook, A. M., Miller, L., Montzka, S., Schwarz, J. P., Sodemann, H., Spackman, J. R., and Stohl, A.: An important contribution to springtime Arctic aerosol from biomass burning in Russia, *Geophys. Res. Lett.*, 37, L01801, doi:10.1029/2009GL041816, 2010. 25287, 25295
- 15 Wespes, C., Emmons, L., Edwards, D. P., Hannigan, J., Hurtmans, D., Saunio, M., Coheur, P.-F., Clerbaux, C., Coffey, M. T., Batchelor, R. L., Lindenmaier, R., Strong, K., Weinheimer, A. J., Nowak, J. B., Ryerson, T. B., Crounse, J. D., and Wennberg, P. O.: Analysis of ozone and nitric acid in spring and summer Arctic pollution using aircraft, ground-based, satellite observations and MOZART-4 model: source attribution and partitioning, *Atmos. Chem. Phys.*, 12, 237–259, doi:10.5194/acp-12-237-2012, 2012. 25285, 25298, 25300
- 20 Wiedinmyer, C., Akagi, S. K., Yokelson, R. J., Emmons, L. K., Al-Saadi, J. A., Orlando, J. J., and Soja, A. J.: The Fire INventory from NCAR (FINN): a high resolution global model to estimate the emissions from open burning, *Geosci. Model Dev.*, 4, 625–641, doi:10.5194/gmd-4-625-2011, 2011. 25289, 25296
- 25 Wild, O. and Akimoto, H.: Intercontinental transport of ozone and its precursors in a three-dimensional global CTM, *J. Geophys. Res.-Atmos.*, 106, 27729–27744, doi:10.1029/2000JD000123, 2001. 25297
- 30 Williams, J. E., van Velthoven, P. F. J., and Brenninkmeijer, C. A. M.: Quantifying the uncertainty in simulating global tropospheric composition due to the variability in global emission estimates of Biogenic Volatile Organic Compounds, *Atmos. Chem. Phys.*, 13, 2857–2891, doi:10.5194/acp-13-2857-2013, 2013. 25333

**Chemical and
physical controls on
pollution transport to
the Arctic**

S. A. Monks et al.

Title Page

Abstract

Introduction

Conclusions

References

Tables

Figures



Back

Close

Full Screen / Esc

Printer-friendly Version

Interactive Discussion



Wofsy, S. C., Sachse, G. W., Gregory, G. L., Blake, D. R., Bradshaw, J. D., Sandholm, S. T., Singh, H. B., Barrick, J. A., Harriss, R. C., Talbot, R. W., Shipham, M. A., Browell, E. V., Jacob, D. J., and Logan, J. A.: Atmospheric chemistry in the Arctic and Subarctic: influence of natural fires, industrial emissions, and stratospheric inputs, *J. Geophys. Res.*, 97, 16731–16746, 1992. 25287

5

Zhang, Q., Streets, D. G., Carmichael, G. R., He, K. B., Huo, H., Kannari, A., Klimont, Z., Park, I. S., Reddy, S., Fu, J. S., Chen, D., Duan, L., Lei, Y., Wang, L. T., and Yao, Z. L.: Asian emissions in 2006 for the NASA INTEX-B mission, *Atmos. Chem. Phys.*, 9, 5131–5153, doi:10.5194/acp-9-5131-2009, 2009. 25289

Chemical and physical controls on pollution transport to the Arctic

S. A. Monks et al.

Title Page

Abstract

Introduction

Conclusions

References

Tables

Figures



Back

Close

Full Screen / Esc

Printer-friendly Version

Interactive Discussion



Table 1. Participating models in inter-comparison. Y in the tracers column indicates that idealised tracers from model have been used for the transport and chemistry analysis in Sect. 5.

Model	Resolution	Meteorology	Chemistry	Tracers	Reference
CAM4-Chem	1.9° × 2.5°, L56	GEOS-5	MOZART-4	Y	Lamarque et al. (2012)
CAM5-Chem	1.9° × 2.5°, L56	GEOS-5	MOZART-4	Y	Lamarque et al. (2012)
C-IFS	T159, L60	ECMWF-Op.	CB05: 55 species, 85 gas-phase reactions Stratosphere: Operational ECMWF O ₃ analysis	Y	Flemming et al. (2012)
GEOS-Chem	2.0° × 2.5°, L47	GEOS-5	~ 100 species HO ₂ gamma for uptake by aerosol set to 1	N	Mao et al. (2010) Parrella et al. (2012)
GMI	2.0° × 2.5°, L72	GEOS-5	based on GEOS-Chem	Y	Strahan et al. (2007) Duncan et al. (2007)
LMDZ-INCA	3.75° × 1.8°, L39	ECMWF-Int	85 tracers, 264 gas-phase reactions Stratosphere: Ozonesonde climatology	Y	Hourdin et al. (2006) Szopa et al. (2013)
SMHI MATCH	0.75° × 0.75°, L35	ECMWF-Int.	63 tracers, 110 gas-phase reactions Stratosphere: Monthly means from EU-MACC project (MOZART-4)	N	Andersson et al. (2007) Robertson et al. (1999)
MOZART-4	1.9° × 2.5°, L56	GEOS-5	103 tracers, 196 gas-phase reactions, Stratosphere: O ₃ constrained by sondes/satellite	Y	Emmons et al. (2010)
TM5	2.0° × 3.0°, L60	ECMWF-Int.	Modified CB05 scheme: 54 tracers, 104 gas-phase reactions. Stratosphere: O ₃ columns nudged to observations	Y	Williams et al. (2013) Huijnen et al. (2010)
TOMCAT	2.8° × 2.8°, L31	ECMWF-Int.	82 Tracers, 229 gas-phase reactions. Stratosphere: 2-D model used for boundary conditions	Y	Monks (2011) Chipperfield (2006)
WRF-Chem	100 and 50 km	WRF	MOZART-4 simulations used as boundary conditions	N	Grell et al. (2005) Fast et al. (2006)

Chemical and physical controls on pollution transport to the Arctic

S. A. Monks et al.

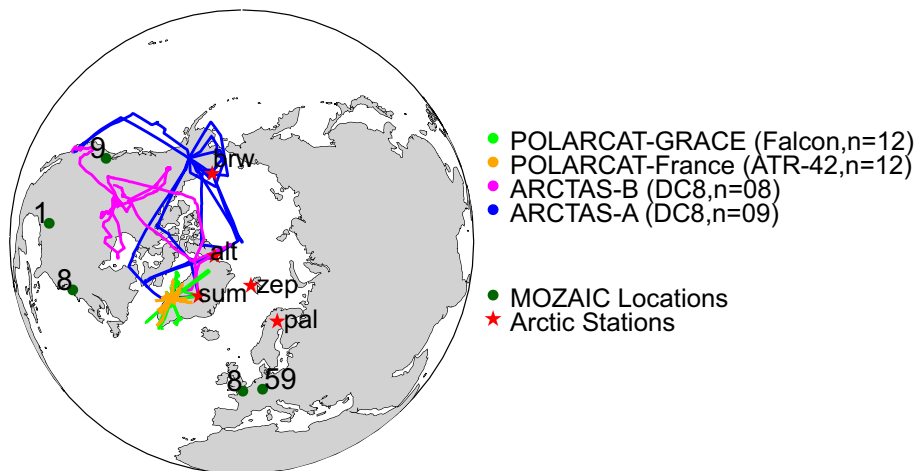


Figure 1. Location of surface stations used for comparisons in Figs. 2–3 (alt = Alert, brw = Barrow, pal = Pallas, sum = Summit, zep = Zeppelin), flight tracks of POLARCAT flights used to calculate vertical profiles in Figs. 7–8 (with n = no. of flights used) and locations of the airports where MOZAIC descent and ascent profiles were used over Europe and North America in Fig. 9 (the values denote the number of profiles at each airport).

Title Page

Abstract

Introduction

Conclusions

References

Tables

Figures

◀

▶

◀

▶

Back

Close

Full Screen / Esc

Printer-friendly Version

Interactive Discussion



Chemical and physical controls on pollution transport to the Arctic

S. A. Monks et al.

Title Page

Abstract

Introduction

Conclusions

References

Tables

Figures



Back

Close

Full Screen / Esc

Printer-friendly Version

Interactive Discussion

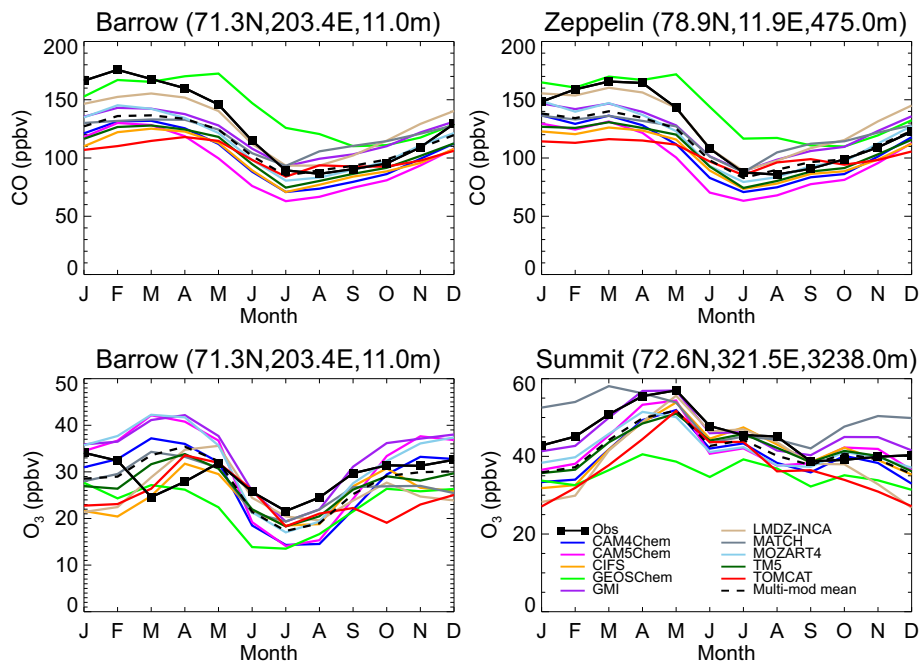


Figure 2. Monthly mean 2008 simulated and observed Arctic surface CO (top) at Barrow and Zeppelin and surface O₃ (bottom) at Barrow and Summit.

Chemical and physical controls on pollution transport to the Arctic

S. A. Monks et al.

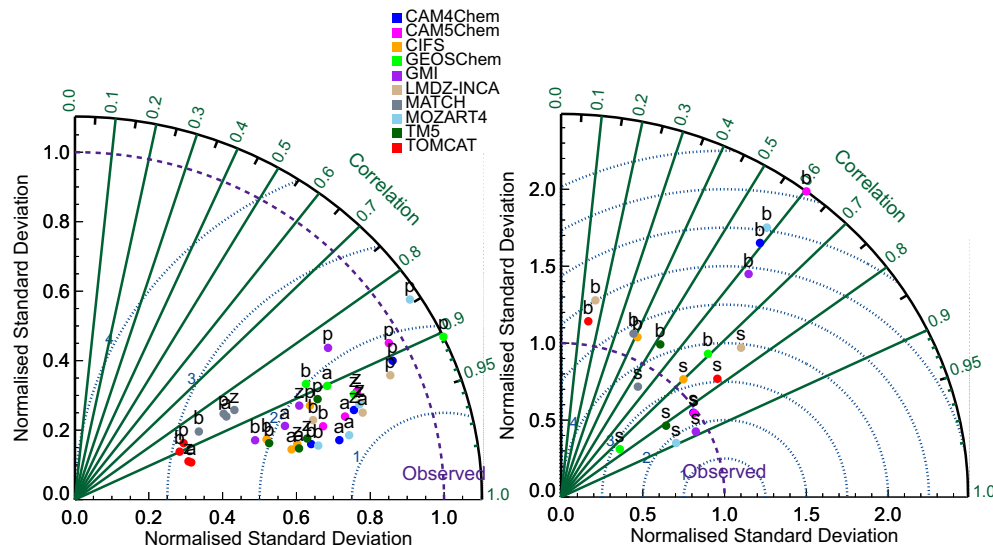


Figure 3. Taylor diagrams for Arctic surface comparisons of monthly mean time series of CO (left) and O₃ (right). Taylor diagrams show the extent to which models capture the observed variability (by the normalised standard deviation (NSD), shown by purple dashed contour), month-to-month changes in concentration (by the correlation (r), shown by green lines) and the mean model bias weighted by the monthly deviations from the annual mean (by the centered root-mean-square difference (RMSD), shown by the black dotted contours). Perfect agreement between a model and observations would result in a NSD of 1, a correlation of 1 and a RMSD of 0, which is indicated by “Observed” on the Taylor diagram. The letters represent the first letter of the station codes shown in Fig. 1.

Title Page

Abstract

Introduction

Conclusions

References

Tables

Figures



Back

Close

Full Screen / Esc

Printer-friendly Version

Interactive Discussion



Chemical and physical controls on pollution transport to the Arctic

S. A. Monks et al.

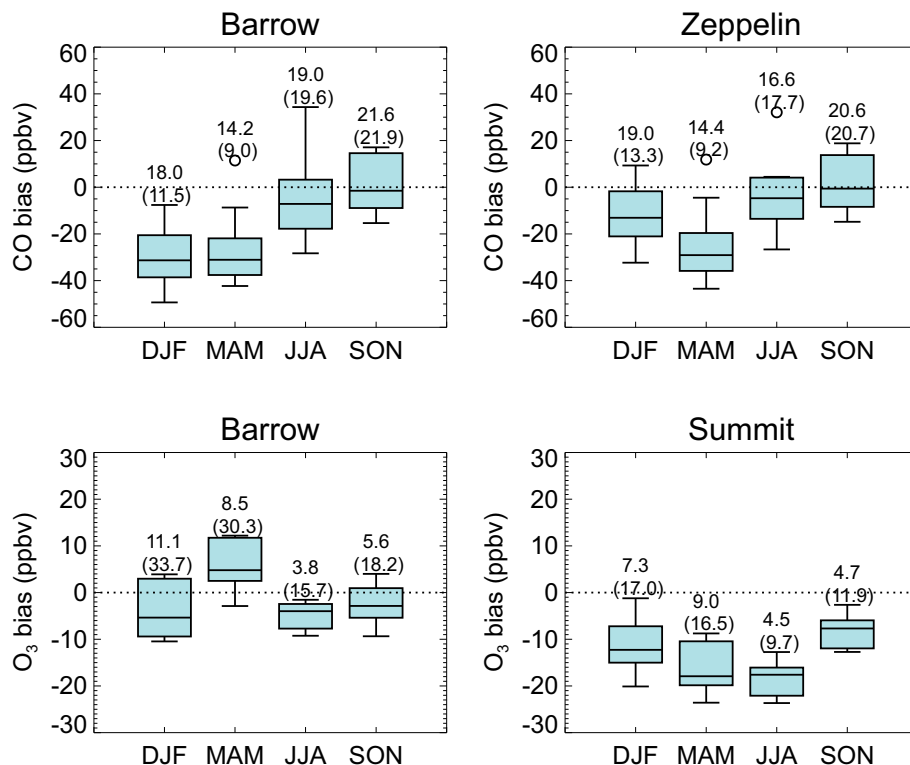


Figure 4. Box and whisker plots showing model seasonal biases (ppbv) for CO at Barrow and Zeppelin (top) and O₃ at Barrow and Summit (bottom). The box and whisker plots show the minimum, 25th percentile, median, 75th percentile and maximum values of the sample. The numbers on the plot represent the interquartile range of each sample (IQR = 75th–25th percentiles) in absolute concentrations and as a percent of observed concentrations (in brackets). Outliers which are more than 1.5 × IQR from the 25th or 75th percentiles are shown by circles.

Title Page

Abstract Introduction

Conclusions References

Tables Figures

◀ ▶

◀ ▶

Back Close

Full Screen / Esc

Printer-friendly Version

Interactive Discussion



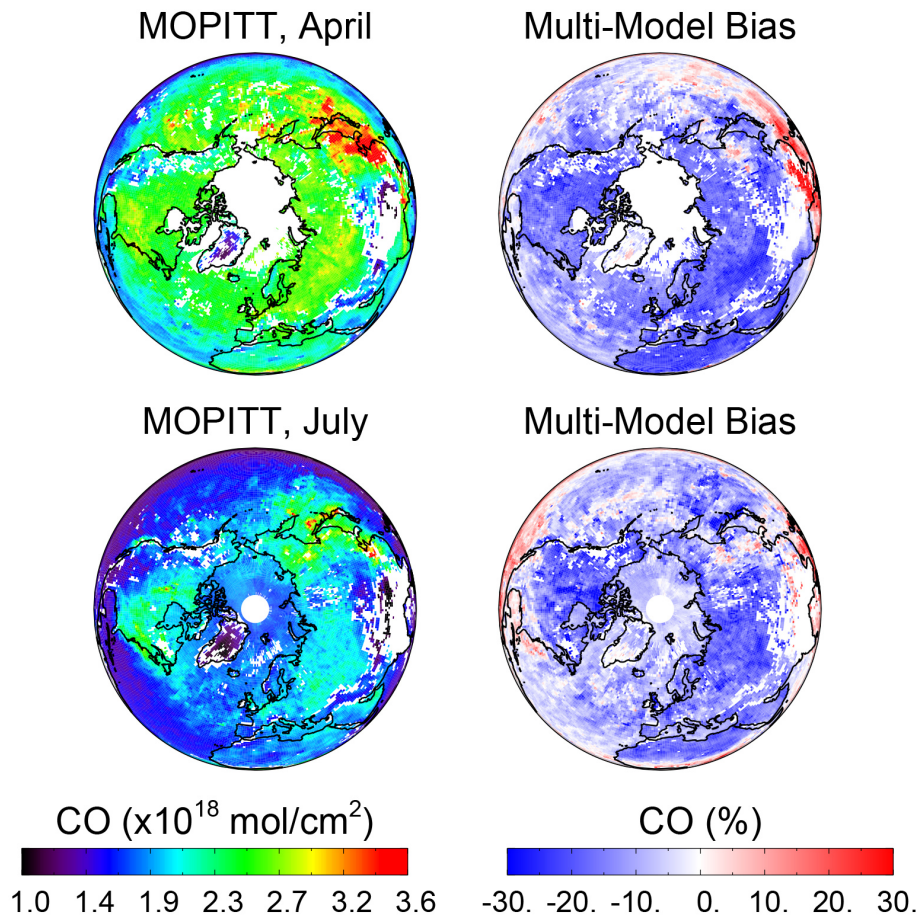


Figure 5. MOPITT total tropospheric CO column (left) and multi-model mean percent bias (right) for April (top) and July (bottom) 2008. The models have had the MOPITT averaging kernels applied and retrievals with DOFS less than 1 have been removed from all data.

Chemical and physical controls on pollution transport to the Arctic

S. A. Monks et al.

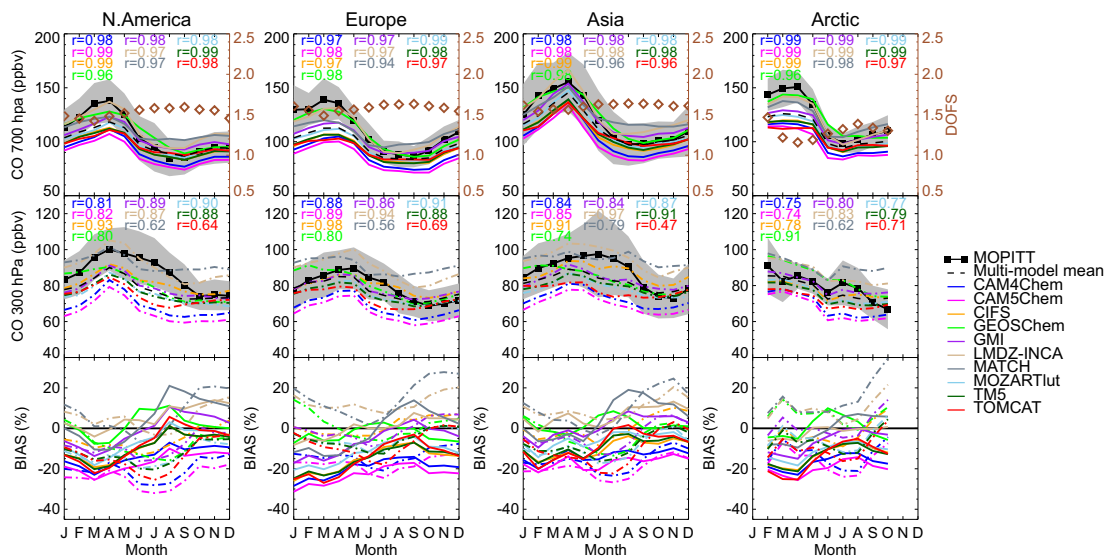


Figure 6. Monthly mean 2008 MOPITT retrieved CO compared to models at 700 hPa (top) and 300 hPa (middle). The monthly mean percent bias (bottom) at 700 hPa (solid lines) and 300 hPa (dashed lines) are also shown. The models have had the MOPITT averaging kernels applied and retrievals with DOFS less than 1 have been removed.

Title Page

Abstract Introduction

Conclusions References

Tables Figures

◀ ▶

◀ ▶

Back Close

Full Screen / Esc

Printer-friendly Version

Interactive Discussion



Chemical and physical controls on pollution transport to the Arctic

S. A. Monks et al.

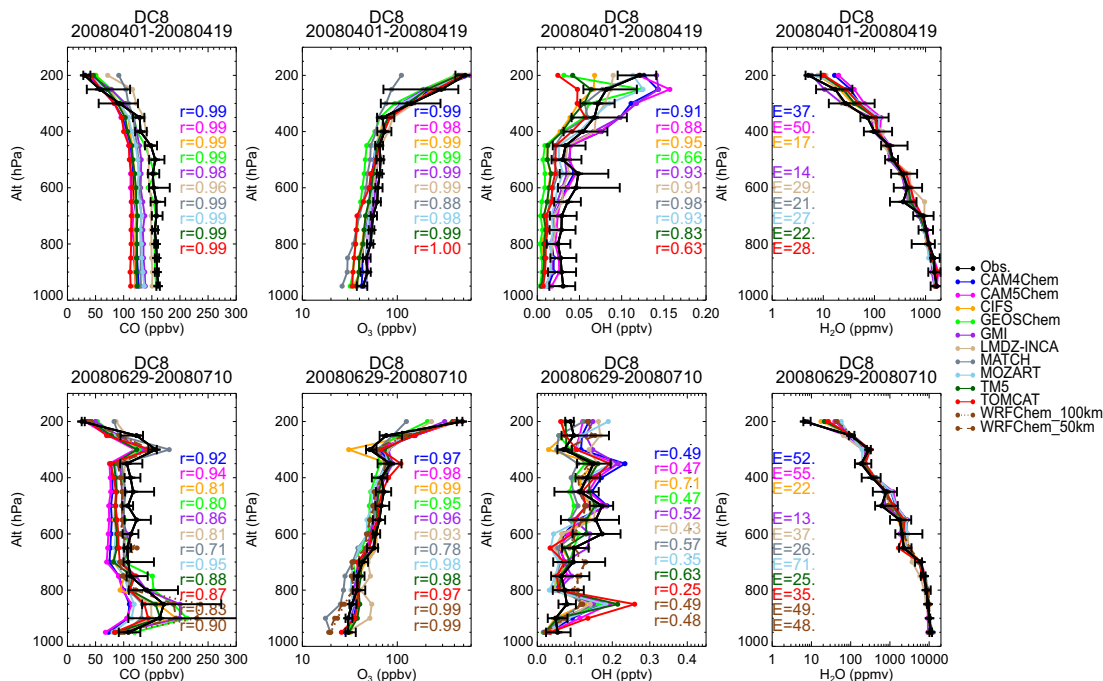


Figure 7. DC8 vertical profiles from the spring ARCTAS-A (top) and summer ARCTAS-B (bottom) campaigns in 2008. Median concentrations of CO (left), O₃ (middle), OH (middle) and H₂O (right), with error bars showing the 25th and 75th percentiles of the observations. Pearson's correlation coefficients are shown for CO, O₃ and OH. NMGE (%) is shown for H₂O. (N.B. Due to missing data in the GEOS-Chem hourly files the median concentrations in the 200, 250 and 300 hPa bins have been calculated over 463 data points instead of 678 data points which are used for the other models and observations.)

Title Page

Abstract	Introduction
Conclusions	References
Tables	Figures

◀
▶

Back	Close
------	-------

Full Screen / Esc

Printer-friendly Version

Interactive Discussion



Chemical and physical controls on pollution transport to the Arctic

S. A. Monks et al.

Title Page

Abstract

Introduction

Conclusions

References

Tables

Figures



Back

Close

Full Screen / Esc

Printer-friendly Version

Interactive Discussion

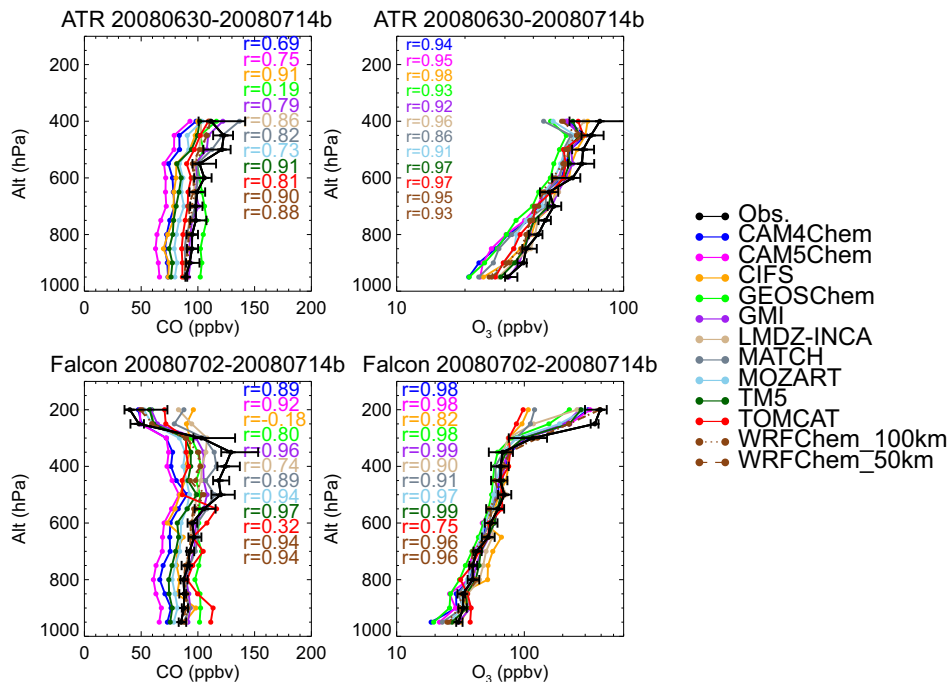


Figure 8. Vertical median profiles from the ATR-42 during the summer POLARCAT-France campaign (top) and the Falcon during the summer POLARCAT-GRACE campaign (bottom) for CO (left) and O₃ (right). Pearson's correlation coefficients are also shown. Error bars show the 25th and 75th percentiles of the observations.

Chemical and physical controls on pollution transport to the Arctic

S. A. Monks et al.

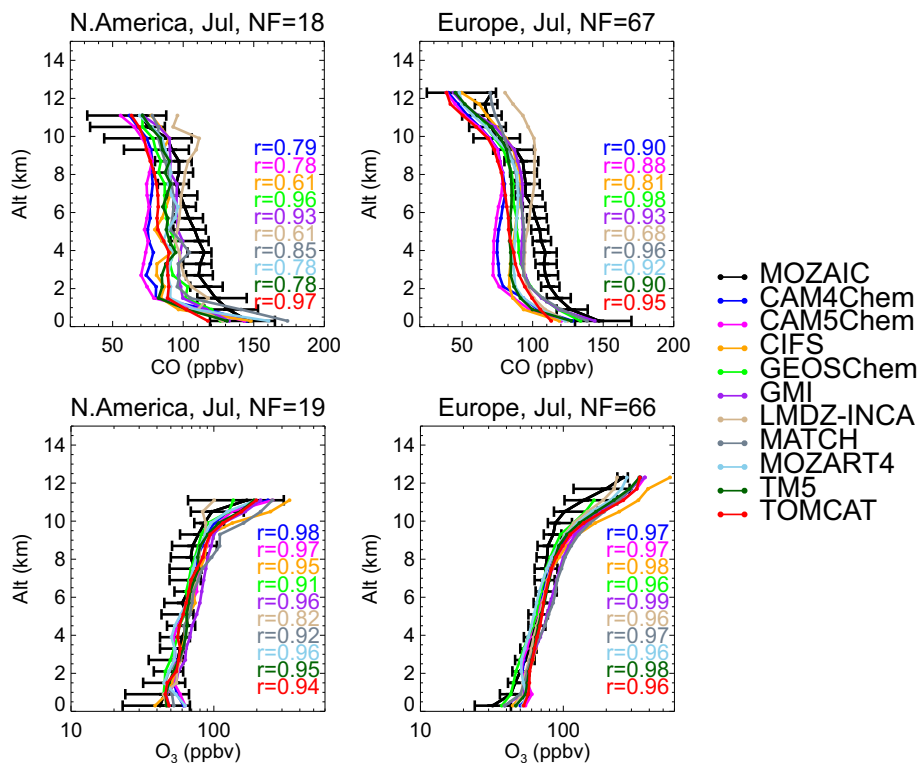


Figure 9. Vertical median profiles from the MOZAIC aircraft project made between 18 June–14 July 2008, during ascent and descent in the regions of North America (left) and Europe (right). Observed CO (top) and O₃ (bottom) are compared to hourly simulated concentrations interpolated to MOZAIC airport location. All data is put into 50 m bins and the error bars show the 25th and 75th percentiles of the observations in each bin. The number of profiles in each location used to calculate the regional profile averages are shown in Fig. 1.

Title Page

Abstract Introduction

Conclusions References

Tables Figures

◀ ▶

◀ ▶

Back Close

Full Screen / Esc

Printer-friendly Version

Interactive Discussion



Chemical and physical controls on pollution transport to the Arctic

S. A. Monks et al.

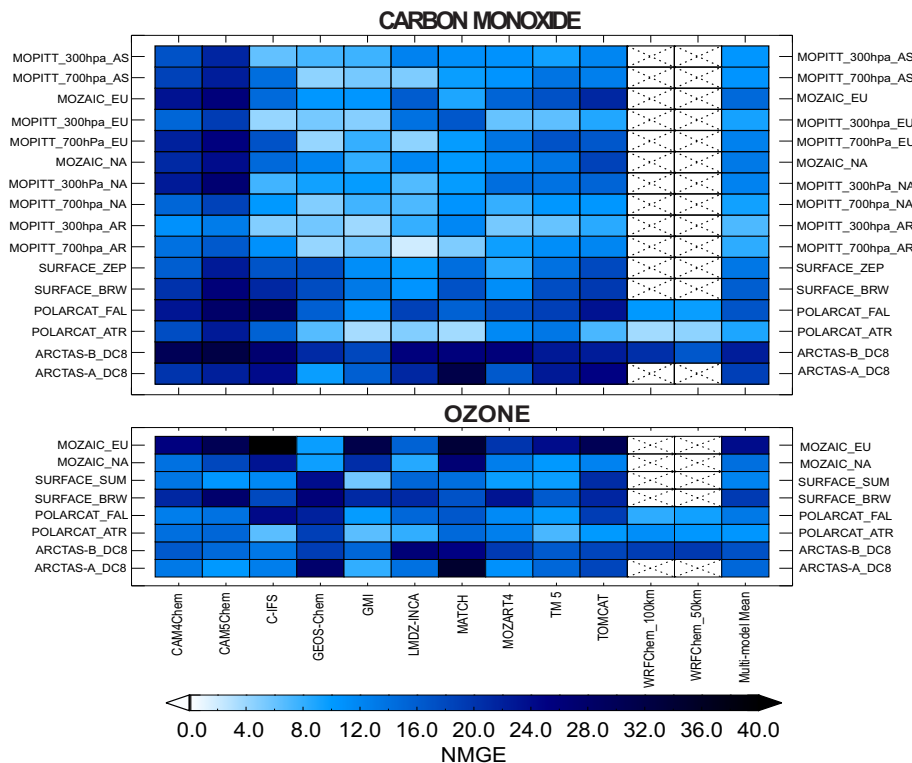


Figure 10. Summary of the Normalised Mean Gross Error ($NMGE = \frac{1}{N} \sum \left(\frac{|mod-obs|}{obs} \right) \times 100$) for all models against observations. The errors are shown for MOPITT regionally averaged satellite retrievals at 300 and 700 hPa (where, EU = Europe, NA = North America, AS = Asia, AR = Arctic), MOZAIC vertical profiles over source regions (where, EU = Europe, NA = North America), at surface sites (where, BRW = Barrow, ZEP = Zeppelin, SUM = Summit) and POLARCAT aircraft observations (where, FAL = Falcon).

Title Page

Abstract

Introduction

Conclusions

References

Tables

Figures



Back

Close

Full Screen / Esc

Printer-friendly Version

Interactive Discussion



Chemical and physical controls on pollution transport to the Arctic

S. A. Monks et al.

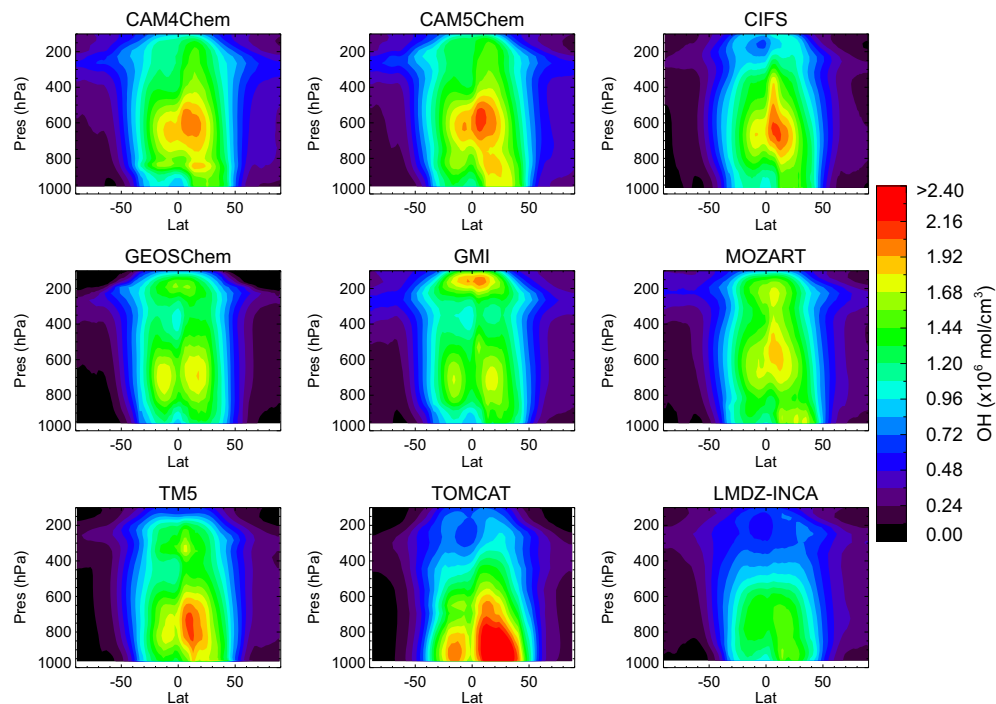


Figure 11. Annual zonal mean OH concentrations ($\times 10^5$ molecules cm^{-3}) for 2008 from the POLMIP models.

[Title Page](#)[Abstract](#)[Introduction](#)[Conclusions](#)[References](#)[Tables](#)[Figures](#)[◀](#)[▶](#)[◀](#)[▶](#)[Back](#)[Close](#)[Full Screen / Esc](#)[Printer-friendly Version](#)[Interactive Discussion](#)

Chemical and physical controls on pollution transport to the Arctic

S. A. Monks et al.

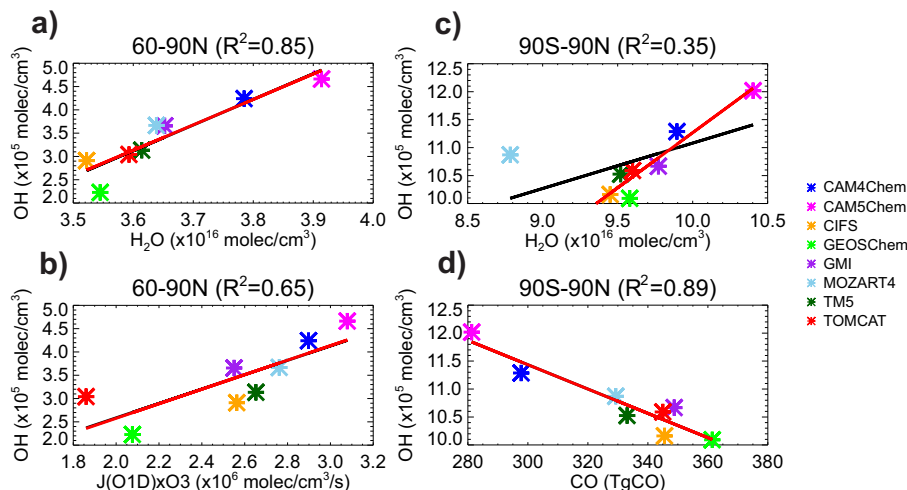


Figure 12. Annual mass-weighted tropospheric mean OH concentration as a function of the **(a)** annual mass-weighted mean water vapour concentration and **(b)** annual mass-weighted mean photolysis rates of $J(\text{O}^1\text{D})$ multiplied by O_3 concentrations in the Arctic, along with the annual mass-weighted global tropospheric mean OH concentration as a function of the **(c)** annual mass-weighted mean water vapour concentrations and **(d)** annual mean total tropospheric CO burden. The ordinary least squares (OLS) and the iteratively re-weighted least squares (IRLS) regression lines are shown in black and red, respectively. Correlations above 0.62 are significant at 90 % confidence level (CL) or above. Removing MOZART from analysis shown in **(b)** results in a r^2 value of 0.91, which is also significant above the 90 % CL. The troposphere has been selected according to the 150 ppbv O_3 contour, however, results are similar when using a climatological tropopause as described by Lawrence et al. (2001). The full list of regression coefficients **(b)** and coefficients of determination (r^2) are shown in Table S1.

Chemical and physical controls on pollution transport to the Arctic

S. A. Monks et al.

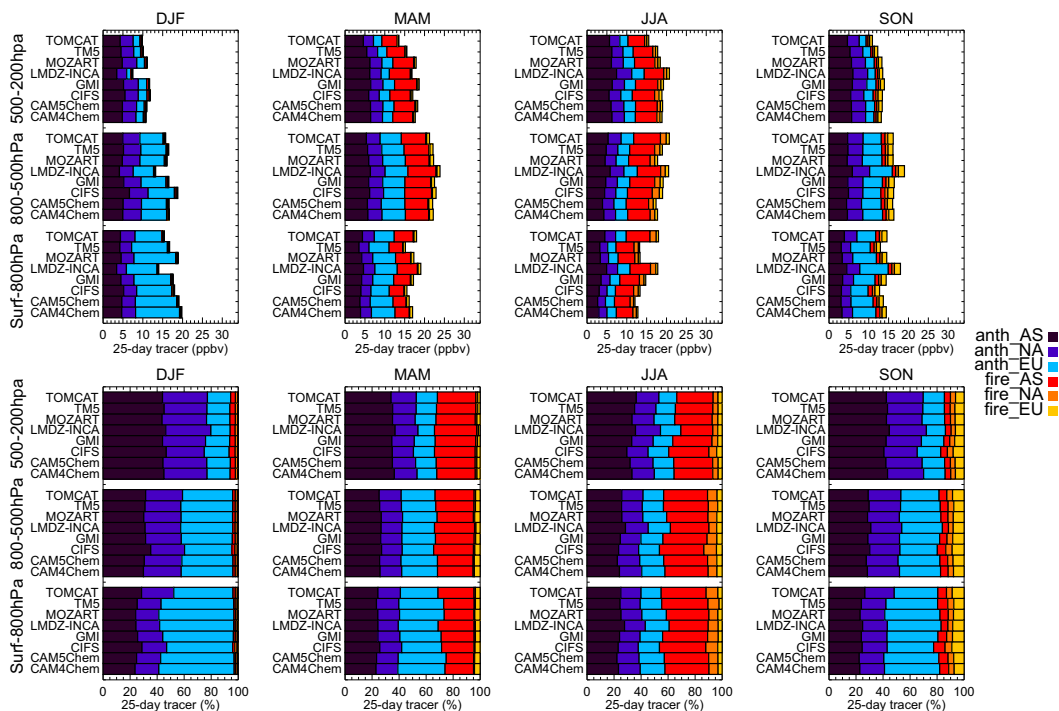


Figure 14. Seasonal mean 2008 regional 25 day fixed loss anthropogenic and biomass burning regional tracers averaged over 3 different altitude bands at latitudes north of 66° N. Contributions shown as absolute concentrations (top) and as a percent of the total CO tracer (bottom). (AS = Asian tracer, NA = North American tracer, EU = European tracer).

Chemical and physical controls on pollution transport to the Arctic

S. A. Monks et al.

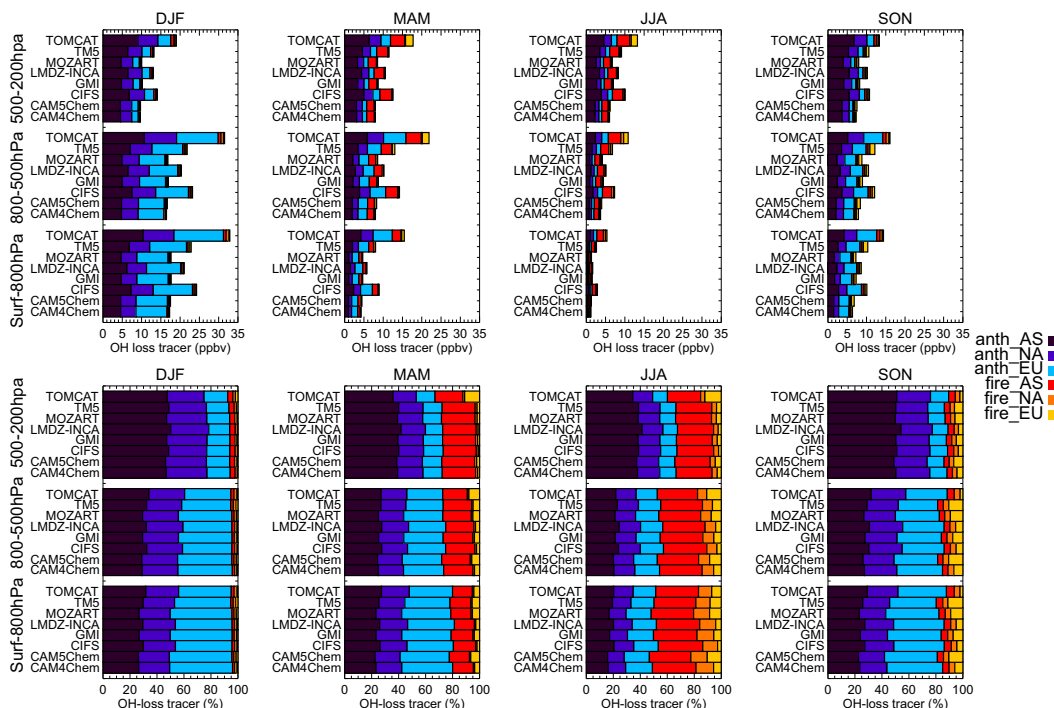


Figure 15. Seasonal mean 2008 regional OH-loss anthropogenic and biomass burning regional tracers averaged over 3 different altitude bands at latitudes north of 66° N. Contributions shown as absolute concentrations (top) and as a percent of the total CO tracer (bottom). (AS = Asian tracer, NA = North American tracer, EU = European tracer).

Title Page

Abstract

Introduction

Conclusions

References

Tables

Figures

⏪

⏩

◀

▶

Back

Close

Full Screen / Esc

Printer-friendly Version

Interactive Discussion



Chemical and physical controls on pollution transport to the Arctic

S. A. Monks et al.

Title Page

Abstract

Introduction

Conclusions

References

Tables

Figures



Back

Close

Full Screen / Esc

Printer-friendly Version

Interactive Discussion

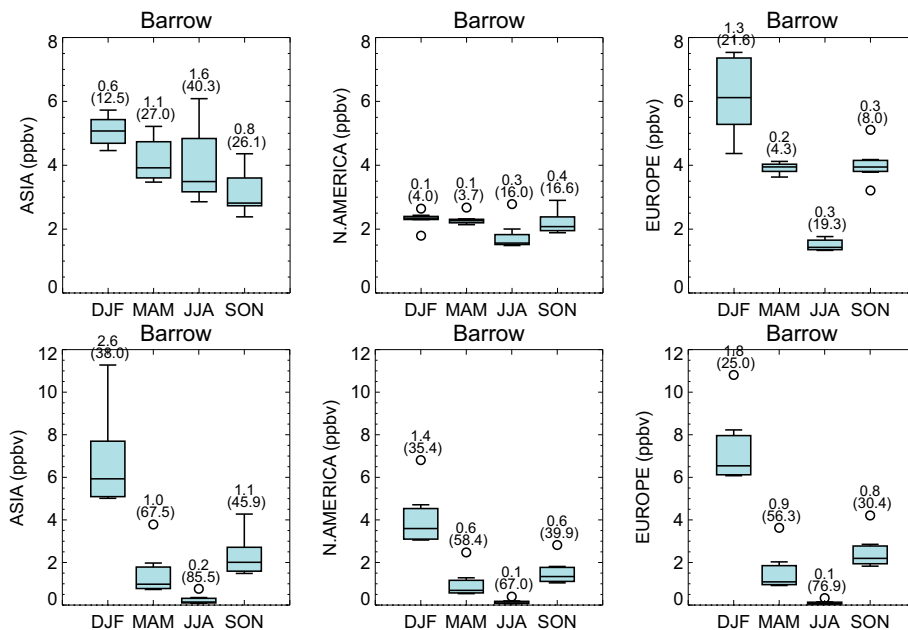


Figure 16. Box and Whisker plots of the anthropogenic 25 day fixed loss tracers (top) and the OH-loss tracers (bottom) at Barrow from 8 POLMIP models. The box and whisker plots show the minimum, 25th percentile, median, 75th percentile and maximum values of the sample. Outliers which are more than $1.5 \times$ IQR from the 25th or 75th percentiles are shown by circles. The numbers on the plot represent the interquartile range as absolute concentrations and as a percent of the multi-model mean (in brackets).

Chemical and physical controls on pollution transport to the Arctic

S. A. Monks et al.

Title Page

Abstract

Introduction

Conclusions

References

Tables

Figures



Back

Close

Full Screen / Esc

Printer-friendly Version

Interactive Discussion



		CO tracers (25-day fixed lifetime)				CO tracers (model OH loss)			
		DJF	MAM	JJA	SON	DJF	MAM	JJA	SON
500-200hPa	anth_AS	0.13	0.11	0.09	0.08	0.27	0.28	0.26	0.23
	anth_NA	0.12	0.08	0.12	0.07	0.22	0.28	0.26	0.22
	anth_EU	0.19	0.13	0.12	0.10	0.27	0.31	0.27	0.25
800-500hPa	anth_AS	0.14	0.06	0.13	0.09	0.32	0.44	0.44	0.34
	anth_NA	0.09	0.02	0.08	0.06	0.25	0.42	0.42	0.29
	anth_EU	0.08	0.04	0.04	0.08	0.19	0.37	0.37	0.23
Surf-800hPa	anth_AS	0.11	0.09	0.22	0.14	0.33	0.62	0.72	0.40
	anth_NA	0.12	0.06	0.15	0.13	0.27	0.58	0.69	0.36
	anth_EU	0.16	0.09	0.14	0.16	0.18	0.48	0.58	0.25

		CO tracers (25-day fixed lifetime)				CO tracers (model OH loss)			
		DJF	MAM	JJA	SON	DJF	MAM	JJA	SON
500-200hPa	fire_AS	0.19	0.11	0.09	0.09	0.29	0.24	0.27	0.31
	fire_NA	0.12	0.08	0.19	0.12	0.31	0.24	0.23	0.23
	fire_EU	0.17	0.25	0.15	0.13	1.00	1.74	1.23	0.29
800-500hPa	fire_AS	0.17	0.07	0.07	0.06	0.39	0.34	0.40	0.37
	fire_NA	0.12	0.07	0.16	0.06	0.32	0.41	0.34	0.27
	fire_EU	0.11	0.12	0.09	0.07	0.43	0.86	0.82	0.40
Surf-800hPa	fire_AS	0.18	0.16	0.14	0.06	0.40	0.52	0.64	0.40
	fire_NA	0.13	0.16	0.23	0.05	0.33	0.62	0.52	0.32
	fire_EU	0.13	0.09	0.20	0.14	0.39	0.61	0.76	0.47

Figure 17. Coefficients of variations ($\frac{\sigma}{\mu}$) calculated from the POLMIP model data binned into altitude bands at latitudes north of 66° N shown in Figs. 14 and 15. The size of the data bars represent the value of the coefficients with anthropogenic coefficients in blue and fire coefficients in red.